AD NUMBER
AD382670
CLASSIFICATION CHANGES
TO: unclassified
FROM: confidential
LIMITATION CHANGES
TO: Approved for public release, distribution unlimited
FROM: Distribution authorized to U.S. Gov't. agencies and their contractors; Administrative/Operational Use; 15 JUN 1967. Other requests shall be referred to Naval Research Labs., Arlington, VA 22203.
AUTHORITY
30 Jun 1979, DoDD 5200.10; NRL ltr, 4 Apr 1981

SECURITY MARKING

The classified or limited status of this report applies to each page, unless otherwise marked.
Separate page printouts MUST be marked accordingly.

THIS DOCUMENT CONTAINS INFORMATION AFFECTING THE NATIONAL DEFENSE OF THE UNITED STATES WITHIN THE MEANING OF THE ESPIONAGE LAWS, TITLE 18, U.S.C., SECTIONS 793 AND 794. THE TRANSMISSION OR THE REVELATION OF ITS CONTENTS IN ANY MANNER TO AN UNAUTHORIZED PERSON IS PROHIBITED BY LAW.

NOTICE: When government or other drawings, specifications or other data are used for any purpose other than in connection with a definitely related government procurement operation, the U. S. Government thereby incurs no responsibility, nor any obligation whatsoever; and the fact that the Government may have formulated, furnished, or in any way supplied the said drawings, specifications, or other data is not to be regarded by implication or otherwise as in any manner licensing the holder or any other person or corporation, or conveying any rights or permission to manufacture, use or sell any patented invention that may in any way be related thereto.

Project Artemis Acoustic Source Performance Characteristics

[Unclassified Title]

R. H. FERRIS AND C. R. ROLLINS

Propagation Branch
Sound Division

June 15, 1957

NAVAL RESEARCH LABORATORY
Washington, D.C.

CONTENTS

ABSTRACT
[Confidential]

The Artemis acoustic source was designed to meet the requirements for an ocean surveillance study program. These requirements included a source level of 152 dB in a 100-Hz band centered at 400 Hz with a transducer operating depth of 1200 feet. The transducer, which was completed in June 1964, is a rectangular planar array 33 feet wide and 50 feet high. It is composed of 1440 variable-reluctance elements which are driven in parallel from a linear electronic amplifier. The source is installed aboard a modified T-2 class tanker having a well amidship through which the transducer array is lowered and retrieved.

Initial tests of the partially completed source had revealed a severe acoustic interaction problem which imposed a restriction on the operating power level. A study program was initiated and experiments were conducted to investigate the interaction behavior and to discover means to alleviate its effects. Results demonstrated that improved performance could be obtained by modifying the original series-parallel connection of elements to an all-parallel form. The indicated modification was performed concurrent with the completion of the transducer array.

Measurements performed on the completed and modified transducer resulted in a set of recommended safe power levels which depend upon frequency. Operation at the recommended maximum power with pulsed sinusoids at 420 Hz, the favorable frequency, produces a source level of 147 dB referenced to one dyne per square centimeter at one yard. Operation at other frequencies is more limited in power, particularly at the upper end of the frequency band.

An acoustic calibration of the source, accomplished with the aid of hydrophones mounted on the end of a 190-foot boom, defined the transfer function in a vertical plane through the acoustic axis out to the first minor lobe. Correlation functions were obtained between the input signal and the acoustic output using pseudorandom signals. It is concluded that the acoustic source introduces negligible distortion in this type of signal.

PROBLEM STATUS

This is an interim report on the Project Artemis acoustic source, work is continuing.

AUTHORIZATION

NRL Problem S02-11
Project ONR RS 046

Manuscript submitted December 28, 1966.

PROJECT ARTEMIS ACOUSTIC SOURCE
[Unclassified Title]

INTRODUCTION

The ocean surveillance study program, Project Artemis, initiated by the Office of Naval Research in 1958, required a very high power, deep acoustic source. The acoustic requirements established for the projector called for a capability of radiating 1000 kW of acoustic power in a 100-Hz band centered at 400 Hz with pulse lengths of 10 to 60 seconds at a 10% duty cycle. Beamwidth to the half-power points was to be 20 degrees in the horizontal plane and 12.5 degrees in the vertical plane. This combination of power and beamwidth would result in a source level of approximately 152 decibels relative to 1 microbar at 1 yard (dB//1 μbar at 1 yd). The acoustic axis was to have a fixed orientation of 11 degrees above the horizontal plane.

Several proposals for the projector were considered, the final selection being a rectangular plane array 33 feet wide by 50 feet high composed of 1440 variable-reluctance transducer elements. Each element is nearly cubical, being 11-1/8 inches square on the radiating face and 11-3/4 inches deep. They are assembled in frames in which 72 elements are closely packed in 12 rows by six columns. Each assembly, referred to as a module, is approximately 6 feet wide by 12 feet high. The completed array consists of four rows of modules with five modules in each row. The modules are mounted on a suitable array frame which provides the proper tilt angle of the radiating face and supports auxiliary components associated with the electrical input to the elements. Radiation to the rear of the array is suppressed by a system of pressure compensated, flattened, gas-filled tubes which serve as acoustic pressure releases on the rear faces of the elements.

A photograph of the completed array is shown in Fig. 1. The array structure is installed in a modified T2-SE-A2 class tanker, the *USNS Mission Capistrano* (T-AG 162). The modification included the installation of a well amidships through which the transducer array can be lowered to depths as great as 1200 feet. When the ship is in transit, the array is stowed within the well. The source ship is equipped with the necessary mechanical equipment for lowering and raising the array and for handling the connecting electrical cables. It also carries suitable electrical power generating equipment and the linear electronic driver for the transducer (1,2).

An initial test (3) of the source facility was conducted in May and June 1961. At that time only two of the projected 20 elements had been installed, as shown in Fig. 2. The purpose of this test was to obtain impedance characteristics, response curves, efficiency, and linearity data. In addition, accelerometers were used to monitor the dynamic displacement of the radiating faces of two of the elements during part of the tests. During the experiment, tests indicated that a number of the transducer elements were damaged. This damage was the result of excessive deflection and subsequent fatigue failure of the transducer element springs. Accelerometer measurements revealed large variations in radiating mass displacements, with the majority in excess of predicted values. These results prompted further tests (4) in June 1961 in which displacement amplitude and phase were monitored at 23 element positions. The results of these and subsequent trials are treated in following sections of this report.

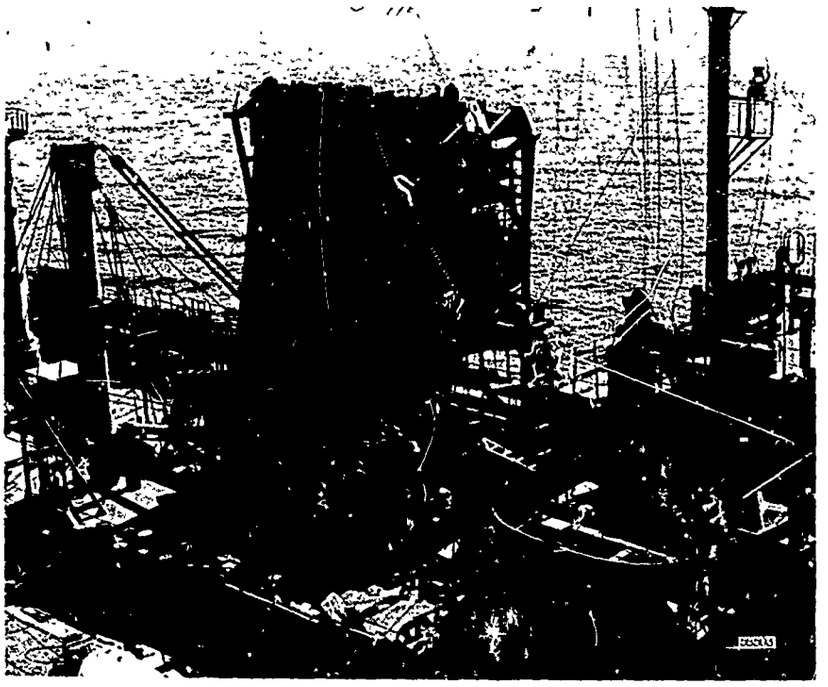

Fig. 1 - The Artemis transducer array

After the initial tests had been completed, the array was enlarged by the installation of 13 additional transducer modules forming three rows of five modules each, as shown in Fig. 3. Evaluation (5) of the larger array configuration was conducted during September and October 1961. While enlarging the array resulted in improved operating characteristics with respect to acoustic loading and displacement distribution, the permissible operating power level was still severely restricted by abnormally high transducer displacements. It became evident that the apparently anomalous behavior was caused by acoustic interaction effects.

A program of experiments (6) and theoretical studies (7) was initiated at this point to further define the interaction problem and to evaluate several possible solutions. The results of this study demonstrated the desirability of changing the electrical drive of the elements from the initial series-parallel conformation to an all-parallel connection. Subsequently, when the array was completed by the addition of the top row of five transducer modules in June 1964, the electrical connection of elements was modified to a parallel connection for the entire array. Tests (8) of the completed and modified array during July 1964 confirmed that a substantial increase in input power capacity had been achieved, although the maximum allowable power was a marked function of frequency. Except for superficial measurements of sound field amplitudes, acoustic tests were deferred pending the availability of an adequate means of positioning the hydrophones stably and accurately in the acoustic field

An acoustic calibration was performed during November 1965. A 190-foot rigid boom pivoted at the base of the array enabled the positioning of monitor hydrophones at

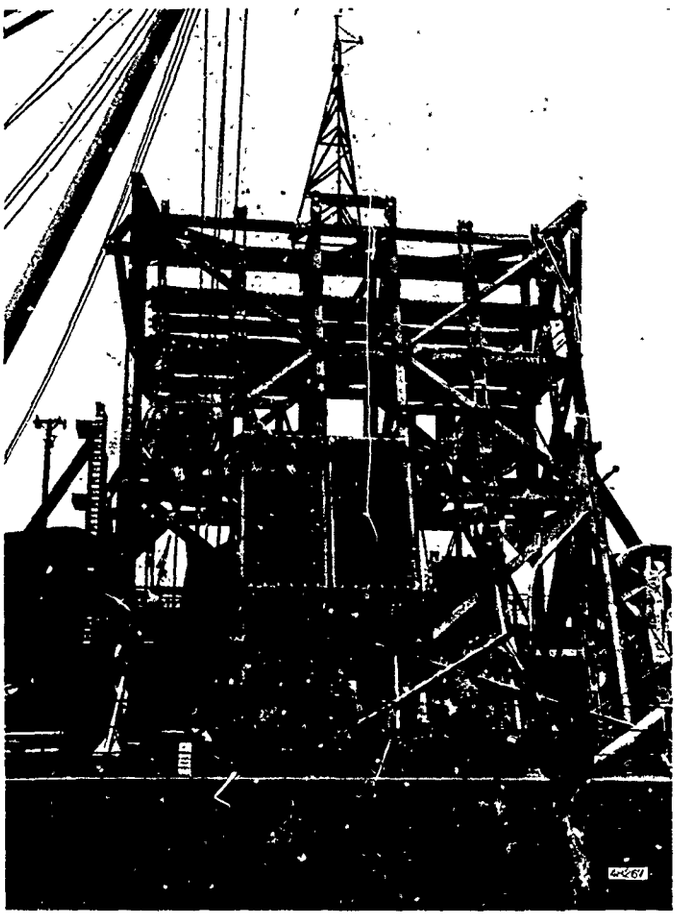

Fig. 2 - The partially completed Artemis array as assembled for initial tests

a selection of positions in a vertical plane through the acoustic axis. Phase and amplitude of the acoustic field were measured with steady-state sinusoidal signals and pseudo-random signals. Crosscorrelations between electrical input and acoustic output were obtained.

This report summarizes the results of all Artemis source tests, including the acoustic calibration which was performed in November 1965. Details of special devices and instrumentation used in the acoustic calibration are described in a separate report (9).

INITIAL TESTS WITH A ONE-WAVELENGTH SQUARE ARRAY

An array composed of 144 variable-reluctance transducer elements was installed on the Artemis array structure in May 1961 for experimentation and determination of operating characteristics. The transducer element which is approximately cubical, being

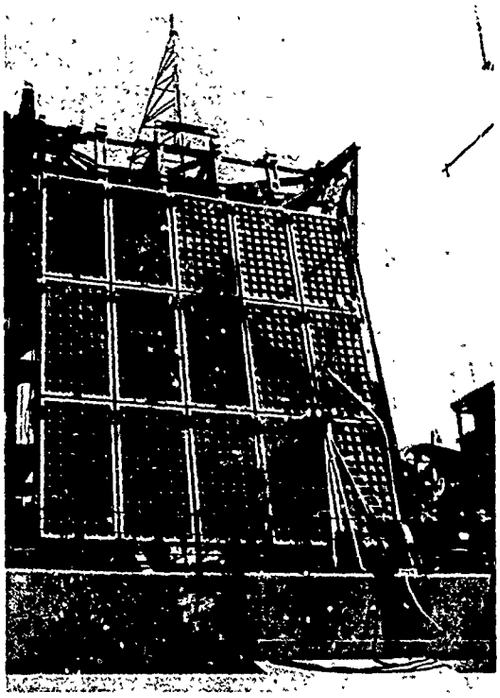

Fig. 3 - The interim 15-module Artemis transducer array

11-1/8 inches square on the radiating face by 11-3/4 inches deep, is a type TR-11C, manufactured to Naval Research Laboratory specification by Massa Division, Dynamics Corporation of America. The transducers were assembled in modules six elements wide by 12 elements high. Two such modules were mounted side by side on the array structure, as shown in Fig. 2. The six elements in each module row were electrically connected in series with the 12 rows connected in parallel. The two modules were then connected in parallel in an oil-filled junction box. Thus, the array consisted of 24 parallel groups of six elements in series. The dc polarizing power, as well as the ac power, was supplied to this group. Each element was polarized with 10 amp of direct current. Acoustic pressure release was provided at the rear (opposite of side shown in Fig. 1) of the modules by flattened-tube resonant reflectors. The tubes were six feet long and extended horizontally across the back of each row of six transducer elements. The flattened tubes were approximately six inches wide, thus covering about one-half of the rear radiating surface of the transducers. The tubes were separated approximately one-half inch from the rear face of the array. In order to prevent the tubes from collapsing under ambient pressure, they were filled with nitrogen gas from a regulated system. The same pressure-release configuration is in use on the present completed array. However, the tubes have been replaced by an improved design and are now filled with dry air rather than nitrogen.

Experimental work with these two modules was conducted during May and June 1961. Two operating areas were used. One was in the Chesapeake Bay near Cape Charles,

Virginia, at a water depth of 90 feet. The maximum possible operating depth to the center of the two modules was approximately 40 feet. The second operating area was in the Atlantic Ocean northeast of the Bahamas at approximately 28°N, 74°W.

Acoustic data were recorded from two monitor hydrophones. One was mounted on a boom which placed it on the center line 28 feet in front of the array. The second hydrophone was also on the center line, 17 feet behind the array. This hydrophone was at the farthest point on the array structure, behind the two modules.

Accelerometers were attached to the radiating faces of two transducer elements in order to monitor displacement amplitudes. In a later experiment, all of the pressure-release tubes were removed to permit attachment of accelerometers to a larger sample of elements. Therefore, although the acoustic data to be presented for this experiment were obtained with pressure-release tubes in place, the displacement data were obtained with the tubes removed, thus allowing radiation both to the front and to the rear.

The array response characteristics and efficiency for a constant input current of 30 amp is illustrated in Fig. 4. The power output was computed from the measured intensity on the acoustic axis and from an assumed directivity index computed for a one-wavelength square piston. The system response for a constant voltage input to the amplifier is shown in Fig. 5. Except for small deviations from smooth curves, the response characteristics appear normal and the efficiency is high. However, during the experiments, tests on the transducer elements indicated that several had failed. These failures apparently were the result of excessive deflections which resulted in failure of the transducer springs. When the displacements of the elements' radiating faces were examined,

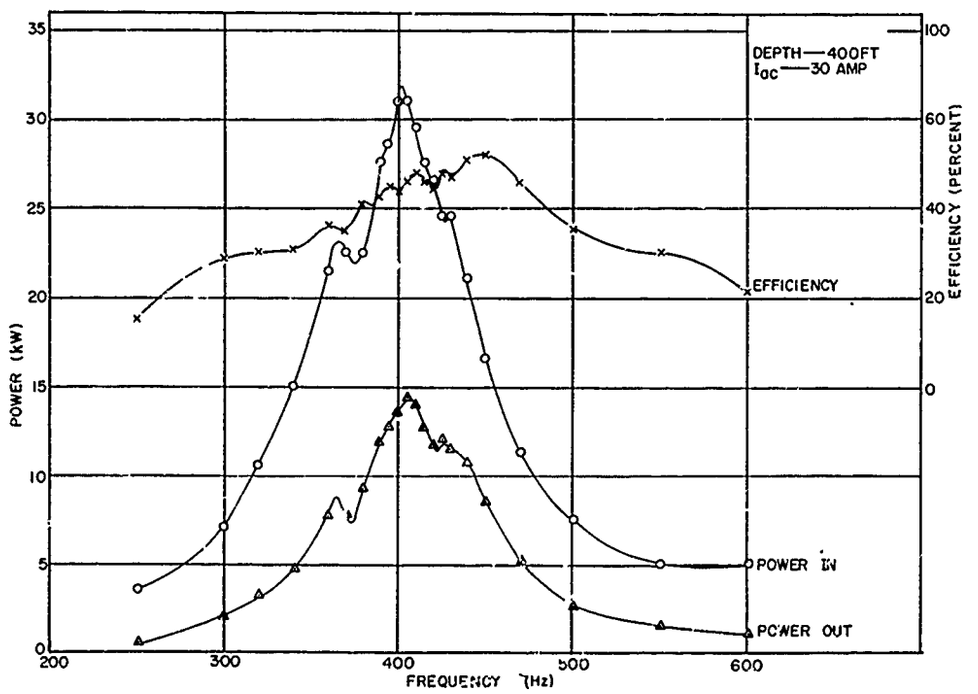

Fig. 4 - Response characteristics of the two-module Artemis array

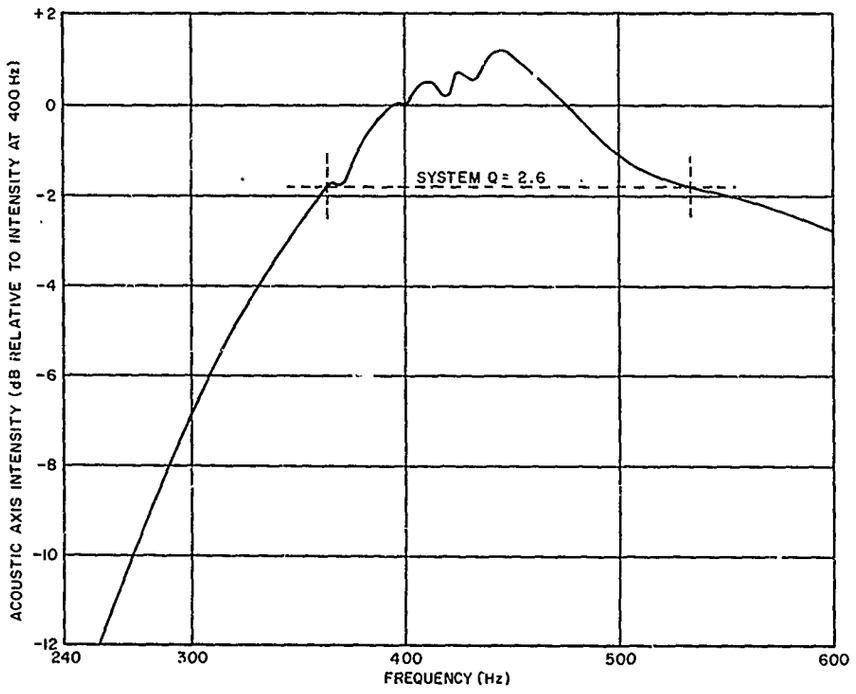

Fig. 5 - Voltage response of the two-module Artemis array, amplifier matched to 34 + j22Ω, transducer current response and impedance data taken at 400 ft depth with I_{ac} = 30 amp

it was apparent that both phase and amplitude had wide variations from element to element and that the pattern was a function of frequency. It is assumed that deviations in the response curves resulted from the variations in element displacement. Typical phase and amplitude patterns for five frequencies within the operating band are illustrated in Fig. 6. The element positions, for which these data were obtained, are those of the first eight elements at the top of the third column from the left, when facing the array. The uppermost element in the column occupies position one. The dashed line in each amplitude plot represents the average value of the data presented in that plot. In an array of displacement-limited elements having a nonuniform displacement distribution, the power input is limited to a value which does not result in a displacement greater than an acceptable value in the element having the largest displacement. Since the displacement is proportional to the square root of the power, an element having double the normal displacement limits the allowable power to one-fourth the normal value for uniform displacements.

At the time of these tests, instrumentation was not available to monitor transducer spring deflections. The transducer springs support a reaction mass, within a watertight housing, which serves as the radiating mass. Fatigue failure of the springs is the factor which limits the operating power level of these elements. Measurement of the outer mass displacement serves as an indication of the uniform behavior of the elements, but it will be shown that there is not a one-to-one correspondence between outer mass displacement and spring deflection.

The effectiveness of the pressure-release tubes was confirmed by comparing the source levels on the axis and reciprocal axis. The results of these measurements, which were performed for various values of input current from 5 to 30 amp, are shown in Fig. 7.

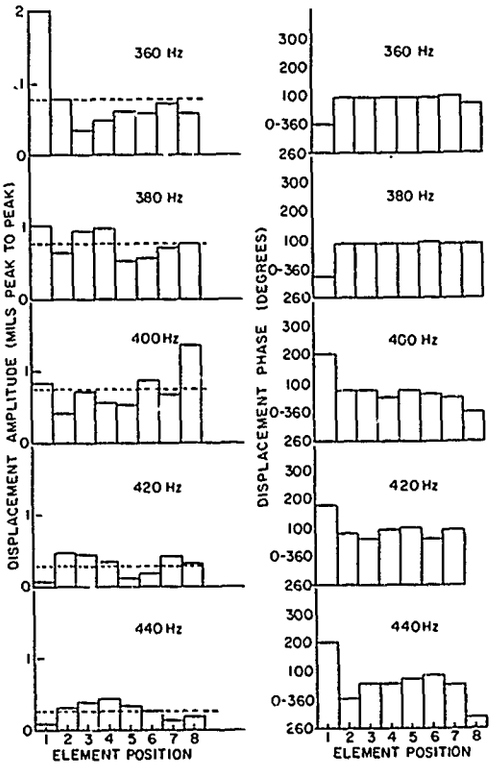

Fig. 6 - Displacement amplitude and phase of the radiating faces for one column of elements in the two-module Artemis array

THE INTERIM 15-MODULE ARRAY

By the summer of 1961 a sufficient number of transducer modules were available to permit enlargement of the array to a configuration of three rows of modules with five modules in each row. A photograph of the array with 15 modules installed is shown in Fig. 3. The installation of the fourth or top row of modules remained to complete the array. The enlarged array was to be used in propagation experiments pending the availability of the last five modules. Four oil-filled component tanks and a junction box were installed in the base of the array structure. The double-armored cables which provide power and instrumentation connections from the ship to the transducer were terminated in the junction box.

Connections are made within the junction box to distribute the power and instrumentation conductors to the four component tanks. The junction box also houses remotely operated contactors which can connect or disconnect power to each tank. Each component tank serves one row of transducer modules and houses the necessary electrical components to appropriately transform and distribute the signal current and the polarizing current to each module in the row it serves. It also contains sensors which measure these currents and transmit the information for remote indication. Polarizing power is transmitted from the ship to the component tanks as three-phase 60-Hz alternating current. A 12-phase silicon diode rectifier in each component tank rectifies the alternating current to provide a 10-amp polarizing current to each of the transducer elements. Each component tank contains a transformer having five secondary windings, which distributes the signal current through appropriate tuning and blocking capacitors to each of the five modules in the row served by that tank. The transformer primaries are connected in parallel in the junction box. Since three rows of modules were installed on the interim array, only three of the four component tanks were used at that time. Pressure release was accomplished at the transducer's rear face in the same manner as in the two-module array.

The array was driven by a 1300-kW linear electronic amplifier. Although only one amplifier was used with the interim 15-module source, four identical amplifiers are

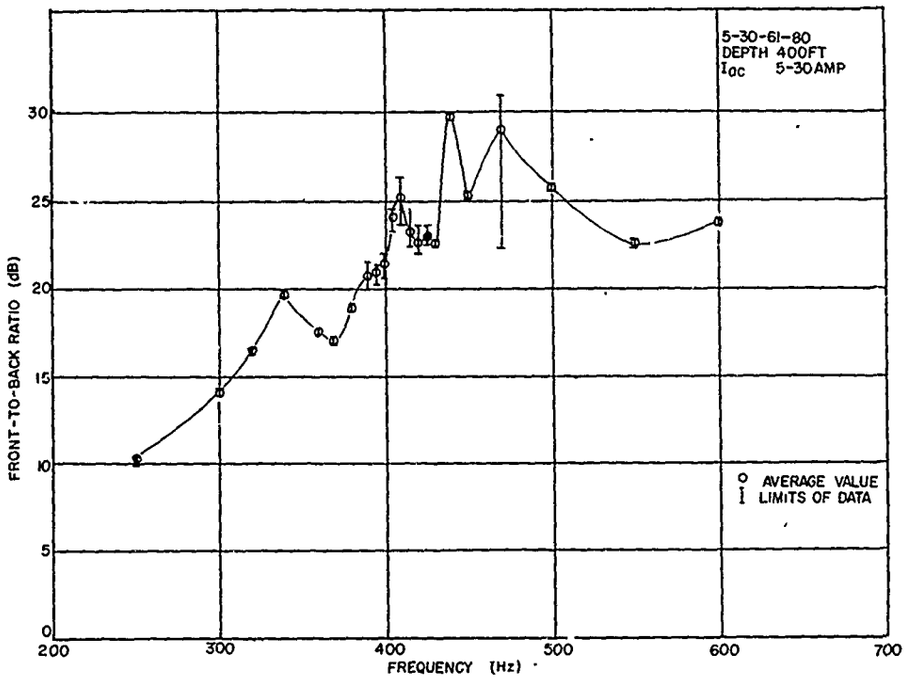

Fig. 7 - Ratio of acoustic pressures in front and to the rear of the two-module Artemis array

available on the ship for driving the completed array. Their outputs can be paralleled in any combination of from one to four amplifiers.

Tests of the 15-module array were conducted in the Cape Charles area of the Chesapeake Bay at a water depth of 80 feet, at 27°28'N latitude and 75°19'W longitude at a water depth of 2540 fathoms, and at various areas within Exuma Sound. The purpose of the shallow-water tests in the Chesapeake Bay was to check the operations of the acoustic source and instrumentation. All data to be presented were obtained in deep water operations.

Thirty-five accelerometers were available for measurement of displacement phase and amplitude. These were moved to sample the displacements of the radiating masses of 81 elements in selected locations, principally in the upper-left-hand quadrant of the array. In addition, one transducer element was specially instrumented with an accelerometer on its inner, or reaction, mass. Current sensors were placed in series with each row of elements in each of two modules. The outputs of the system current sensors, which monitor the ac and dc currents to each module, were also available. Crude acoustic measurements were obtained by suspending a hydrophone from a small boat at a range of approximately 60 yards. The hydrophone was moved in azimuth and depth until a maximum response indicated a position on the acoustic axis. The range was measured acoustically.

With steady-state sinusoidal drive, the current was measured in each of the 12 rows of elements in the module located in the geometrical center of the array. Figure 8 illustrates the results at each of 15 discrete frequencies. An approximately sinusoidal pattern with a repetition interval equal to the sound wavelength in water is apparent. Theoretical studies of the radiation loading, as modified by acoustic interactions, show a similar pattern having acoustic load maximums spaced at approximately one-wavelength intervals across the face of an array. It is very probable that acoustic loading patterns resulting from interactions are responsible for the variations in current with element position. However, the data illustrated in Fig. 8 are somewhat complicated by the fact that the current in each row is determined by the loading on a row of six series-connected elements. Thus, variations of element displacement throughout the array are partly due to acoustic loading interactions and partly to electrical impedance interactions.

The distribution of displacement amplitude and phase was more uniform in the enlarged array than in the two-module array. However, peak displacements were still much larger than those predicted for a fully loaded, uniformly vibrating piston producing the same power output. This was particularly evident in the upper half of the frequency band. The elements to which accelerometers were attached are marked with X's in the diagram of Fig. 9. In the four following illustrations, rows of elements are numbered from the top and columns from the left. Figures 10a and 10b illustrate the displacements observed in two instrumented rows and one instrumented column of elements at frequencies of 400 Hz and 430 Hz, respectively. Corresponding diagrams of phase are illustrated in Figs. 11a and 11b. These are typical of patterns observed at other frequencies with a noted tendency for less uniform patterns in the upper half of the frequency band. Again, interpretation of the phase and amplitude data is complicated by the series-parallel connection of elements. As was previously noted, the displacement amplitude of

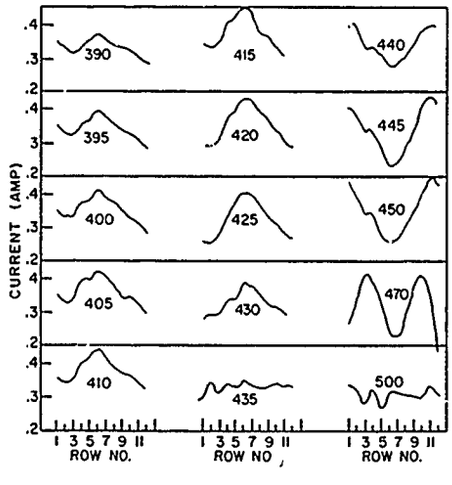

Fig. 8 - Current distribution in series-connected rows of elements in one module of the 15-module Artemis array

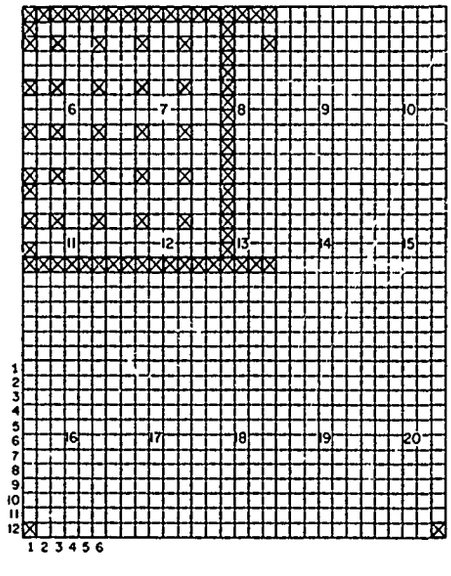

Fig. 9 - Accelerometer locations (marked with crosses), module identification, and element row and column enumeration for the 15-module Artemis array

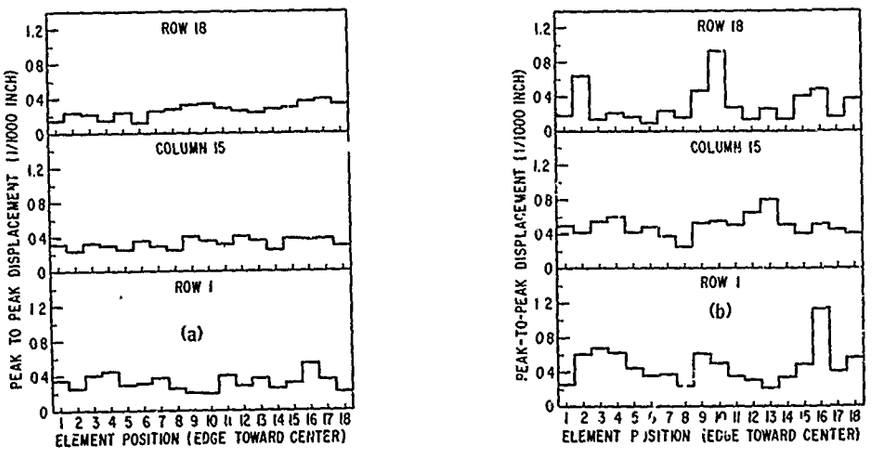

Fig. 10 - Displacement amplitude patterns for the 15-module array

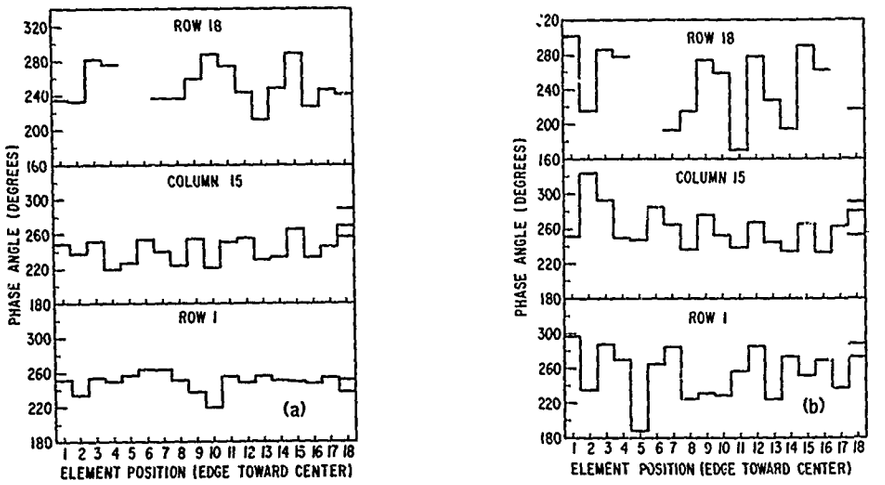

Fig. 11 - Displacement phase patterns for the 15-module array

the radiating mass cannot be directly related to power limitation, since it is the transducer spring deflection which limits power. Figures 12 and 13 illustrate the observed relations of inner and outer mass displacement and phase, respectively, for an element position near the center of the array. These data were obtained with the specially instrumented element containing an accelerometer on the inner mass. Since the transducer springs are between the inner and outer masses, the vector sum of the mass displacements is equal to the spring deflection. It is apparent that there is not a one-to-one relation between outer mass displacement and spring deflection as the frequency is varied. Only one specially instrumented element was available for this test, and it was therefore impractical to obtain a wide sampling of spring deflections over the elements of the

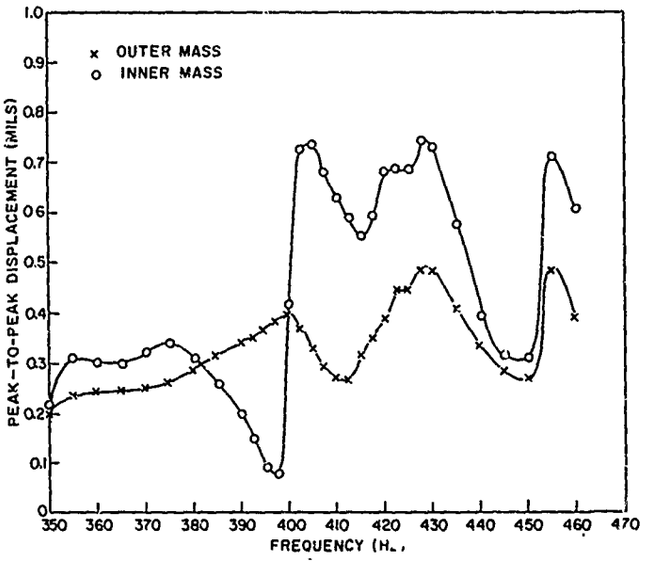

Fig. 12 - Displacement amplitude of the inner and outer masses for one element in the 15-module array

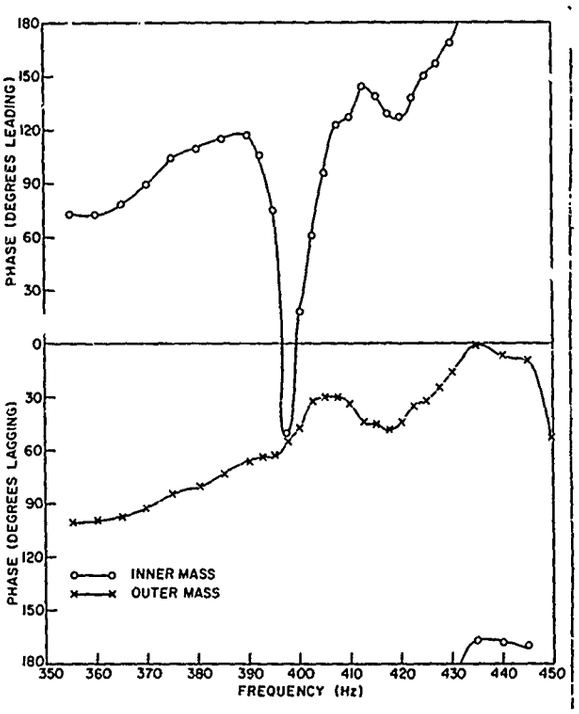

Fig. 13 - Displacement phase of the inner and outer masses for one element in the 15-module array

array. Quantitative limits on power, therefore, were not available. The wide variation in outer mass displacements, however, revealed an unsatisfactory operating condition.

Results of this test, which disclosed a severe interaction problem, prompted the initiation of an experimental and a theoretical program to gain a better understanding of the problem and to develop a technique for coping with interactions in the Artemis array.

ACOUSTIC INTERACTIONS

A series of tests were conducted to investigate the effectiveness of three techniques for reducing the effects of acoustic interaction on the velocity distribution among elements in the Artemis array. The first method consisted of bonding a group of elements into a subassembly to effectively increase the size of the unit element. This should have the effect of increasing the self-acoustic loading of the unit element and thus reduce the relative contribution of the interaction loading. A minimum element size of one-half-wavelength square was indicated by the work of Rusby (10). The second approach was to use a parallel electrical connection of transducer elements as opposed to the series-parallel configuration of the original array. The parallel connection permits a current distribution in which the current through an element is inversely proportional to the element impedance; thus, an element with high electrical impedance resulting from low acoustic loading caused by the interaction field would receive a lower drive current than an element with low impedance resulting from high loading. In the original series-parallel configuration the current through an element was controlled by the total impedance of six series-connected elements and thus was not subject to the self-limiting action inherent in an all parallel connections. The third technique used parallel connected elements which were individually tuned by means of series capacitors to reduce the susceptibility to variations in loading. This method has been shown to be effective in an array of piezoelectric projectors by Carson, et al. (11).

The first test series was conducted during May 1962 in the Cape Charles area of the Chesapeake Bay at a water depth of 90 feet. Operations were performed aboard the *USS Hunting* (EAG 398), a Laboratory research vessel, the experimental array being lowered through a well amidships. The experimental array for this test series consisted of a nominally one-wavelength square array of 144 elements. Subassemblies of transducer elements were fabricated by mechanically bonding the sides of several elements together to make a single larger radiating element. There were three such subassemblies, one of 36 elements in a six-by-six configuration, and two of 12 elements in three-by-four configurations. The remaining spaces in the transducer array were filled by individual elements. Nine elements each in the upper-right-hand and lower-left-hand quadrants of the 36 element assembly were modified by the addition of accelerometers attached to the inner masses. Each of the 18 elements was provided with two internal accelerometers, one at the top edge and one at the bottom edge of the inner mass. In addition, each of the 36 elements in the subassembly was modified by the addition of a stainless steel slug inserted in the lower face on the cable entrance end of each element. This slug was centered below an existing slug in the center of each transducer face and, like the existing slug, was provided with a tapped hole to which an accelerometer could be attached. Thus, provision was made for monitoring the displacement at two points on the outer mass of each of the 36 elements and at two points on the inner mass of each of 18 elements. Each of the 12 elements in one of the smaller subassemblies was similarly instrumented, as were three of the individual elements. Suitable electric cables were provided to permit a series-parallel connection as in the Artemis array, or an all-parallel connection of any group of 36 elements.

The second test series was conducted during July 1962 at the Navy Electronics Laboratory Pend Oreille Calibration Station at Bayview, Idaho. Two experimental arrays, each approximately one-half wavelength square, were investigated. One array was the 36-element consolidated subassembly used in the Chesapeake Bay tests, whereas the other consisted of 36 unconsolidated elements. The unconsolidated array contained 18 specially instrumented elements of the same type and in the same configuration as in the consolidated array. The 36 elements in each array were connected in parallel by means of transformers and 36 extension cables. Provisions were made for inserting tuning capacitors in series with each element. As in the Chesapeake Bay tests, flattened, gas-filled tubes were installed approximately 8 inches behind each row of elements to suppress acoustic radiation to the rear. Details of the experimental procedures for both test series are presented in Ref. 5.

The effect on the uniformity of outer mass displacement of electrical connection, individual tuning, and consolidation of elements is shown in Figs. 14a through 14d. In these figures the average values of displacements are shown as circled points, whereas the range of observed values is indicated by the shaded region. All values in Figs. 14a through 14c have been normalized to 1 kW electrical input power. Values in Fig. 14d have been normalized to 1 kW acoustic power. Figure 14a, which illustrates the characteristics of the series-parallel, unconsolidated configuration, serves as a reference to evaluate the degree of improvement. Figure 14b illustrates the improvement in displacement uniformity obtained by the use of an all-parallel electrical connection. When the individual elements were tuned by inserting a 5 μF capacitor in series with each element, the effects shown in Fig. 14c were obtained. Tuning resulted in an improved distribution at the upper end of the frequency band with a slight worsening at some other frequencies. Consolidation of the elements, with the results shown in Fig. 14d, tended to reduce the spread of the displacement data. However, the maximum values were not reduced at all frequencies.

It was previously pointed out that the transducer spring deflections in the TR-11 element are not directly related to outer mass displacement. Examples of the spring deflections observed in these tests are illustrated in Figs. 15a through 15d. Again, the circled points represent average values and the shaded area represents the range of values. Spring deflections in the control group, that is, the series-parallel, unconsolidated configuration, are shown in Fig. 15a. Figures 15b, 15c, and 15d illustrate the effects of parallel connection, tuning, and consolidation as indicated in the figures. The high values of spring deflection observed in the consolidated group at frequencies in the neighborhood of 370 Hz result from a nonrectilinear, or rocking, motion of the inner mass. This mode of oscillation, while present in all groups, is accented by consolidation.

The average acoustic powers per element which would result in spring deflections of 10 mils peak to peak were computed for the various test configurations. Figures 16 and 17 illustrate the results of these computations. It can be observed that the parallel connection of unconsolidated elements, without individual tuning, yields the best overall results. Although individual tuning effects an improvement at the upper end of the frequency band, the improvement, when considering the band as a whole, is marginal.

The results of this test were extrapolated to predict the improvement to be expected if the full 2-1/2 by 4 wavelength Artemis array were modified to an all-parallel electrical interconnection and the elements either group tuned or individually tuned. The predicted source levels are plotted in Fig. 18, along with the source level for the series-parallel configuration.

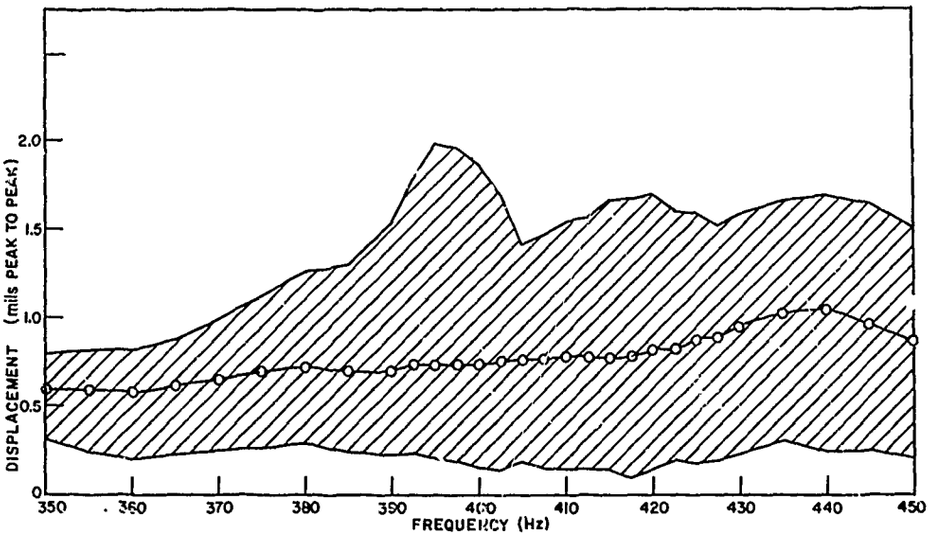

Fig. 14a - 36-element unconsolidated group in $\lambda \times \lambda$ array, series-parallel connection, displacement values normalized to 1 kW electrical power. Circled points indicate average values, shaded area indicates range of values.

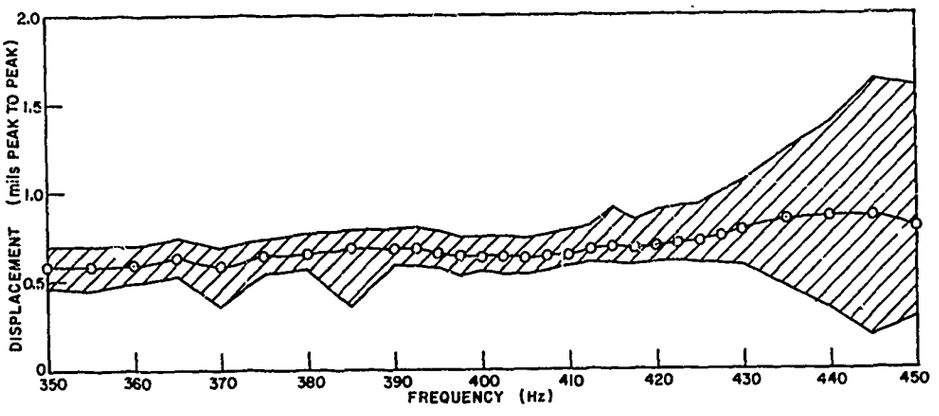

Fig. 14b - Same as above with "series-parallel connection" changed to: parallel-group tuned connection

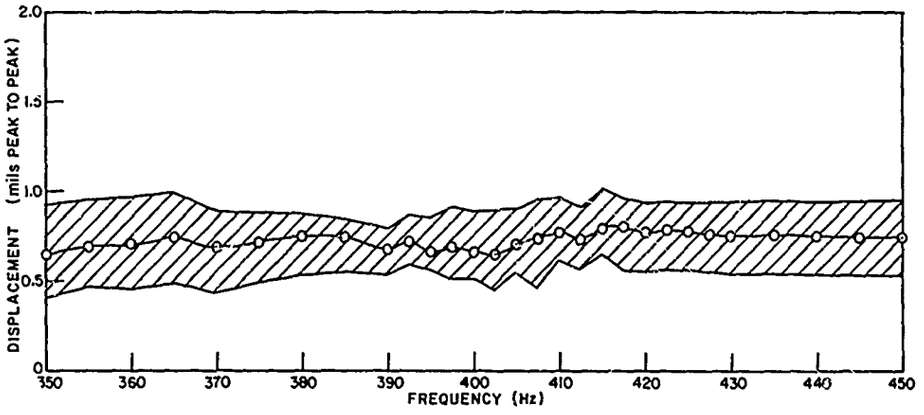

Fig. 14c - Same as 14a with "series-parallel connection" changed to: parallel-individually tuned (5 μF) connection

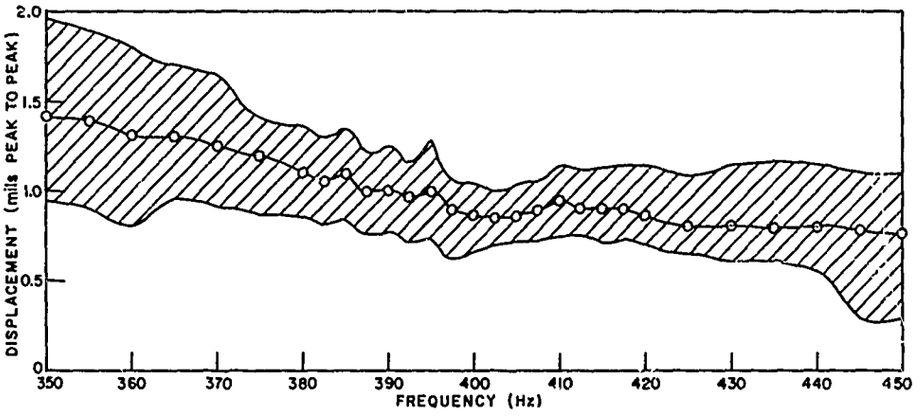

Fig. 14d - 36-element consolidated array, parallel-group tuned connection, displacement values normalized to 1 kW acoustic power. Circled points indicate average values, shaded area indicates range of values.

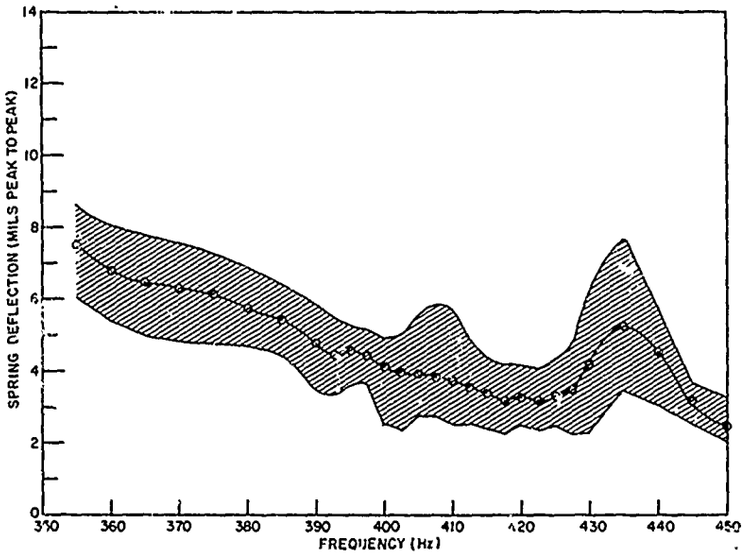

Fig. 15a - 36-element unconsolidated group in $\lambda \times \lambda$ array, series-parallel connection, group tuned, values normalized to 1 kW electrical power. Circled points indicate average values, shaded area indicates range of values.

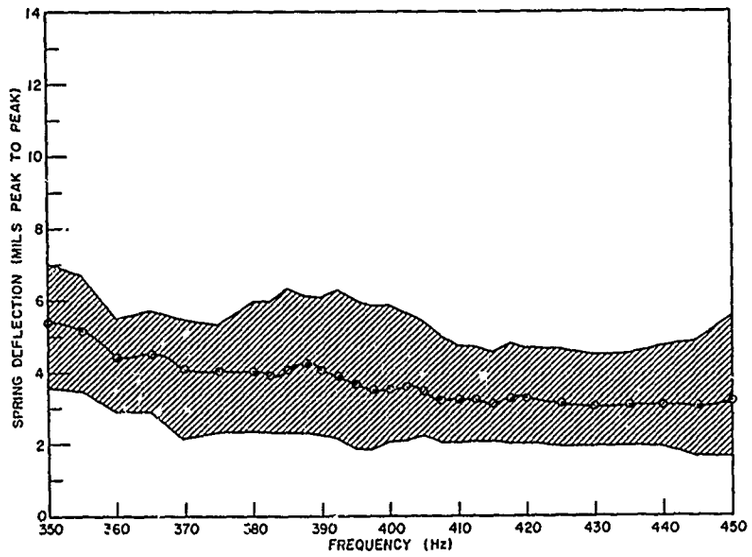

Fig. 15b - 36-element unconsolidated array, parallel-group tuned connection, values normalized to 1 kW acoustic power. Circled points indicate average values, shaded area indicates range of values.

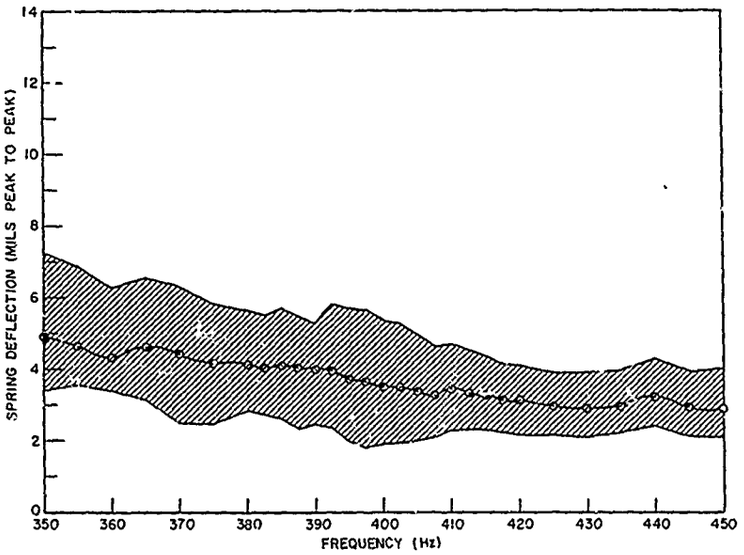

Fig. 15c - Same as 15b with "parallel-group tuned connection" changed to: parallel-individually tuned (5 μF) array

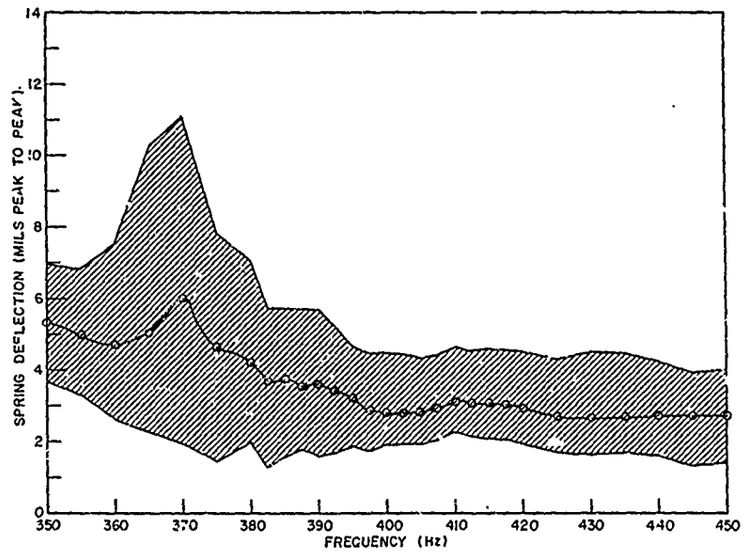

Fig. 15d - Same as 15b with "unconsolidated" changed to: consolidated

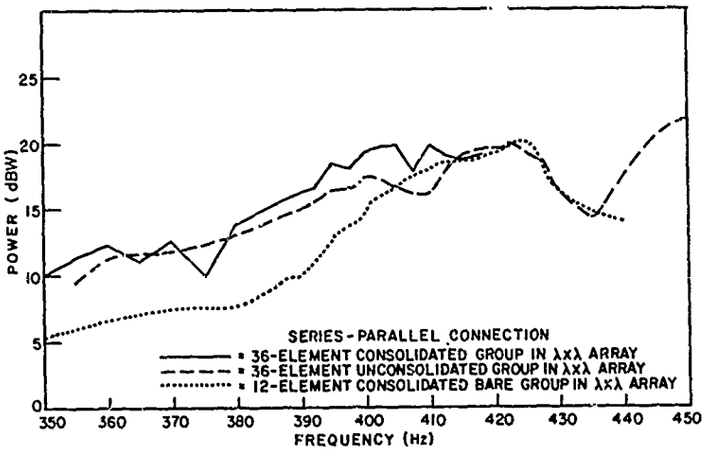

Fig. 16 - Average acoustic power per element with array limited to a maximum spring deflection of 10 mils peak to peak

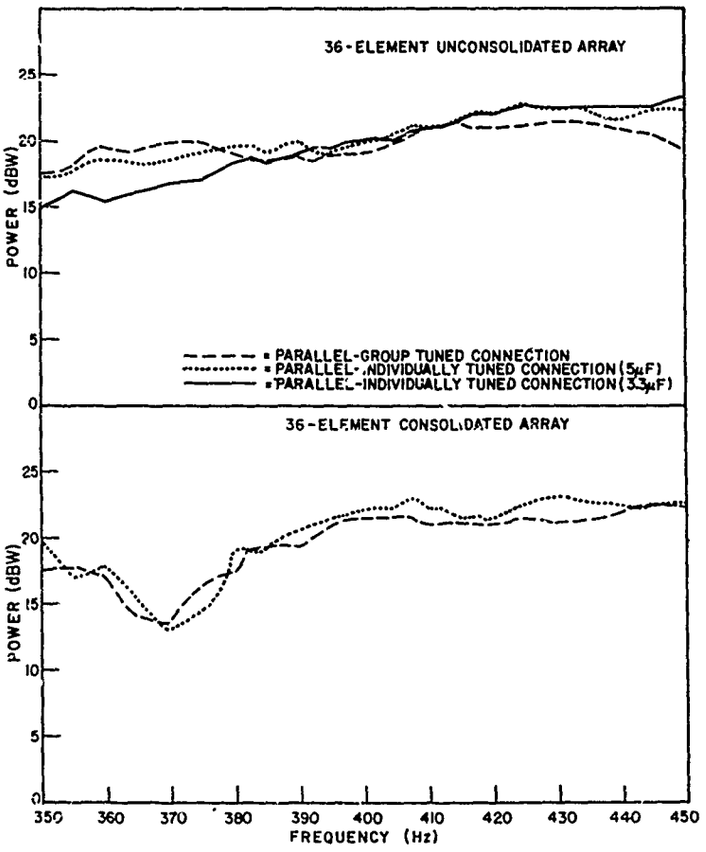

Fig. 17 - Average acoustic power per element with array limited to a maximum spring deflection of 10 mils peak to peak

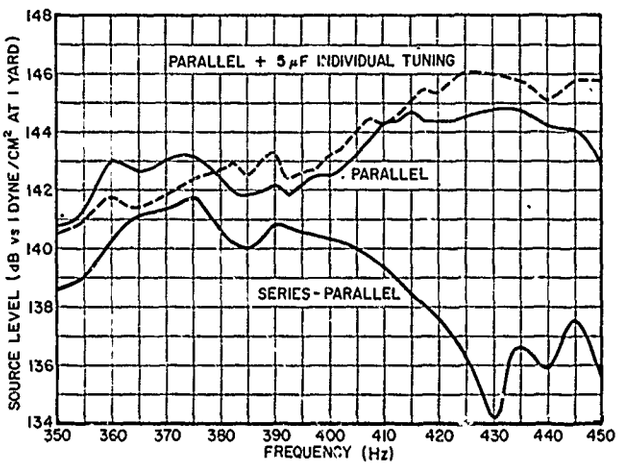

Fig. 18 - Predicted source levels of the full Artemis array for three configurations of electrical connection of elements

A theoretical study (7) in which the transducer array was simulated on a digital computer also confirmed that an all-parallel connection of elements would improve performance. It also predicted that individual tuning of elements would increase the allowable power at the upper end of the frequency band.

As a result of the studies and experiments, the decision was made to modify the electrical connection of elements in the Artemis array to an all-parallel configuration.

PERFORMANCE OF THE COMPLETED ARRAY

Power Tests of the Completed and Modified Source

In the spring of 1964 the transducer array was completed by adding the top row of five transducer modules, resulting in a rectangular plane array 33 feet wide and 50 feet high. Concurrent with the installation of the additional transducer elements the electrical connection to all elements was modified from the previous arrangement, in which groups of six elements were connected in series and all series groups connected in parallel, to the present configuration, in which all elements are connected in parallel. This was accomplished by installing paralleling transformers on the array structure to the rear of each transducer module. The transformers are required to preserve the impedance compatibility between the transducer modules and existing circuitry. The squashed tubes, which provide pressure-release backing for the elements, were also replaced by tubes of an improved design having an increased radius of curvature at the bends. A number of the previous tubes had suffered fatigue failure, and it was thought that they would not withstand the anticipated higher intensity acoustic field which could be generated by the modified source.

Tests to determine the operating characteristics and the allowable level of power of the modified and completed source were conducted in Northwest Providence Channel in July 1964. One specially instrumented transducer module, containing 32 of the elements

which had been modified by the installation of internal and external accelerometers, was installed in module position two, that is, the second position from the left in the top row when facing the front of the array. During the tests the special module was moved sequentially to positions 8, 14, 20, and 11, as shown in Fig. 19. Positions of the instrumented elements within the test module are indicated by the cross-checked areas. At each position the array was driven with continuous waves, the current being held constant as the frequency was stepped over the operating band. Spring deflections were computed from the recorded inner and outer mass displacement of each instrumented element. In addition, provision was made for summing the inner and outer mass displacements for five of the instrumented elements in order to monitor spring deflections of those elements when the array was driven by broadband signals. Array impedance was computed from the measured voltage, current, and power input. The array was submerged to a depth of 600 feet during these tests.

The resistive and reactive components of array impedance are plotted in Fig. 20. The impedance data were obtained at a constant current of 50 amp except at frequencies higher than 445 Hz, where it was reduced to 25 amp.

The mean and maximum observed spring deflections for continuous wave excitation are illustrated in Fig. 21. The distributions of spring deflections, which have been divided by the mean at each frequency, are plotted for eight illustrative frequencies in Fig. 22. It can be observed from both of these plots that there is a wide spread between

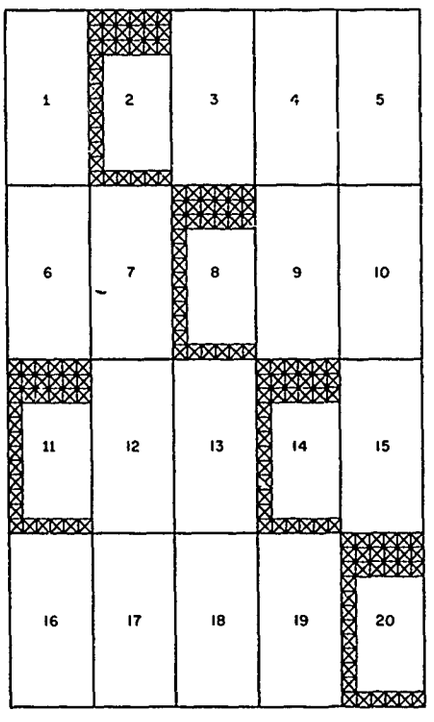

Fig. 19 - Arrangement of instrumented elements (marked by crosses) during tests of the completed Artemis array

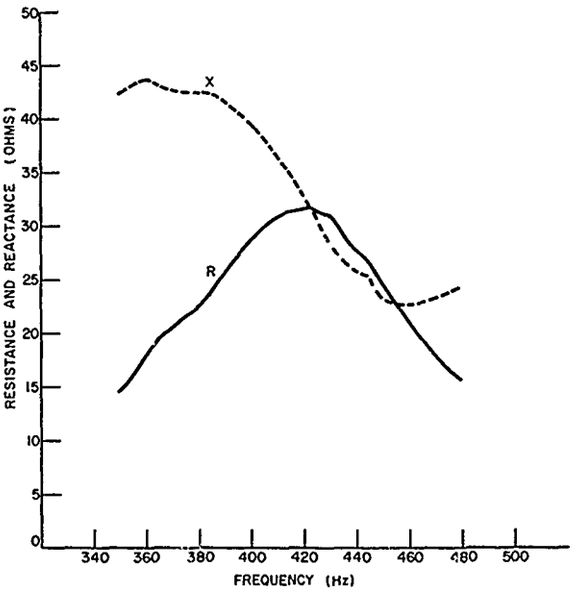

Fig. 20 - Resistive and reactive impedance components for the completed Artemis array

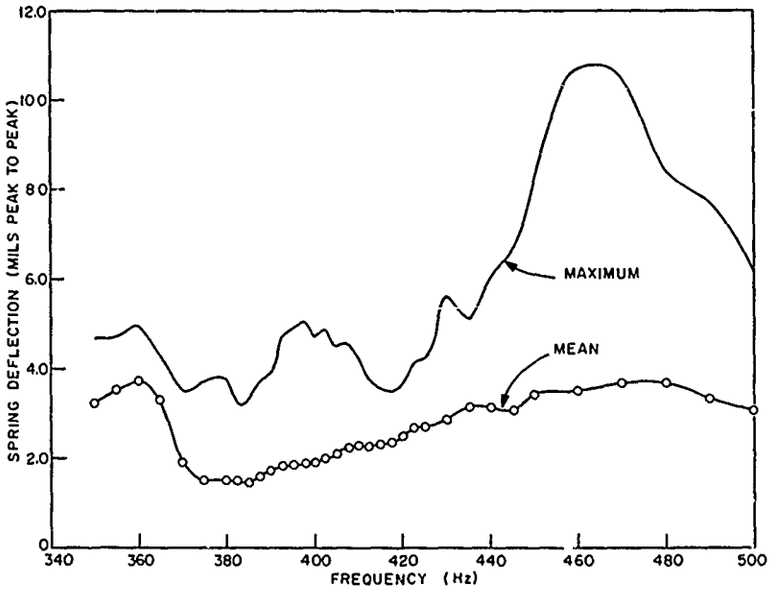

Fig. 21 - Mean and maximum observed spring deflections with continuous-wave excitation for the completed Artemis source

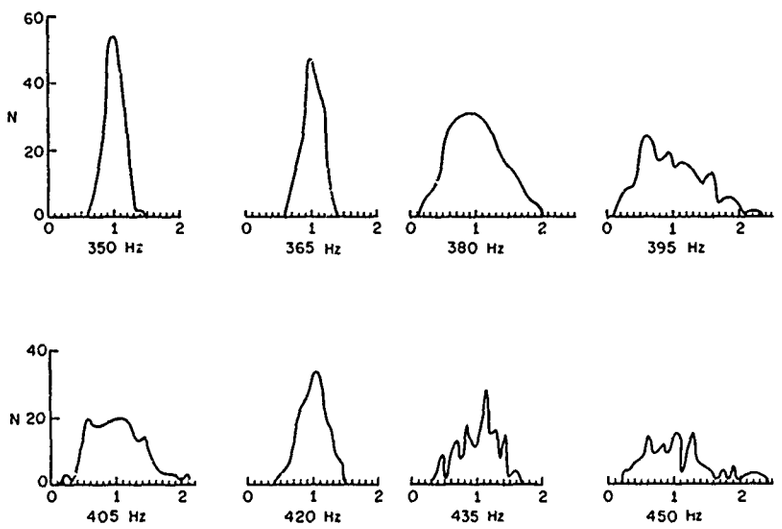

Fig. 22 - Distribution of spring deflections in the completed Artemis source

the maximum and the mean at frequencies of 380, 395, 435, and 450 Hz. The divergence above 430 Hz is a consequence of the element response to variations in acoustic loading. When a constant voltage is applied across the input terminals of a single unloaded element measured in air, the spring deflections vary with frequency in the manner illustrated in Fig. 23. A sharp maximum occurs at the impedance pole. If the element were loaded with a mass reactance, the frequency at which the deflection maximum occurs would decrease. If a resistive load were added, the principal effect would be a reduction in the height of the maximum. When an element is operating in an array, it experiences wide variations in acoustic loading due to acoustic interactions. Figure 24 (7) illustrates how the real part of the radiation load can vary, relative to unity ρcA loading, over the face of a uniform-velocity array. The data illustrated were computed for one quadrant of a 2-1/2 by 4 wavelength uniform-velocity array, i.e., equal amplitude and phase over the array face, at a frequency of 400 Hz. The reactive component of loading has a similar pattern. If an element is in a position to experience a large mass reactive load, the spring deflection peak illustrated in Fig. 23 would occur within the operating band and would have a height dependent upon the value of the resistive component of loading. At frequencies below that at which the pronounced peak deflection occurs, it can be shown (8) that the value of spring deflection is relatively insensitive to the character of the radiation load. It is the effect described above which causes the marked nonuniform distribution of spring deflections at frequencies above 430 Hz, as shown in Figs. 21 and 22. It can be seen from Fig. 22 that the distributions at frequencies of 380, 395, and 405 Hz are also very broad. This results from a resonance in a rotary mode (8) of vibration of the inner mass. This mode produces large spring deflections without a correspondingly large displacement of the outer mass and, hence, does not contribute to the acoustic field.

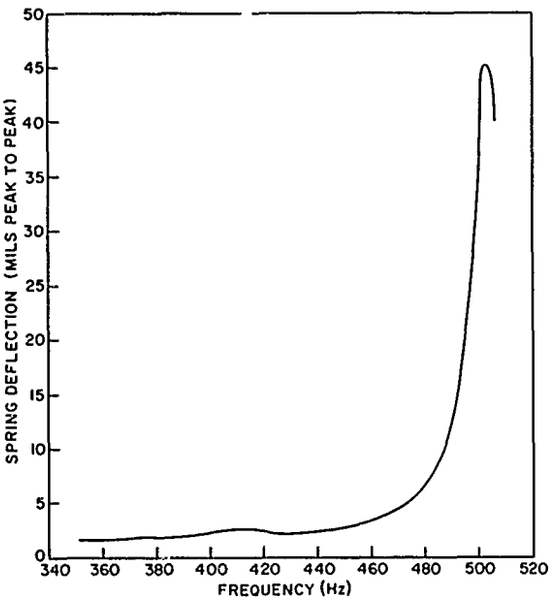

Fig. 23 - Spring deflections of an unloaded element in air for a constant-voltage drive

2 1/2λ BY 4λ
ONE QUADRANT OF ARRAY
EQUAL VELOCITY
ka ELEMENT DIMENSION ~ 0.24
kx ~ 7.73
ky ARRAY DIMENSIONS ~ 12.37
AIR RESONANT FREQUENCY ~ 0.27

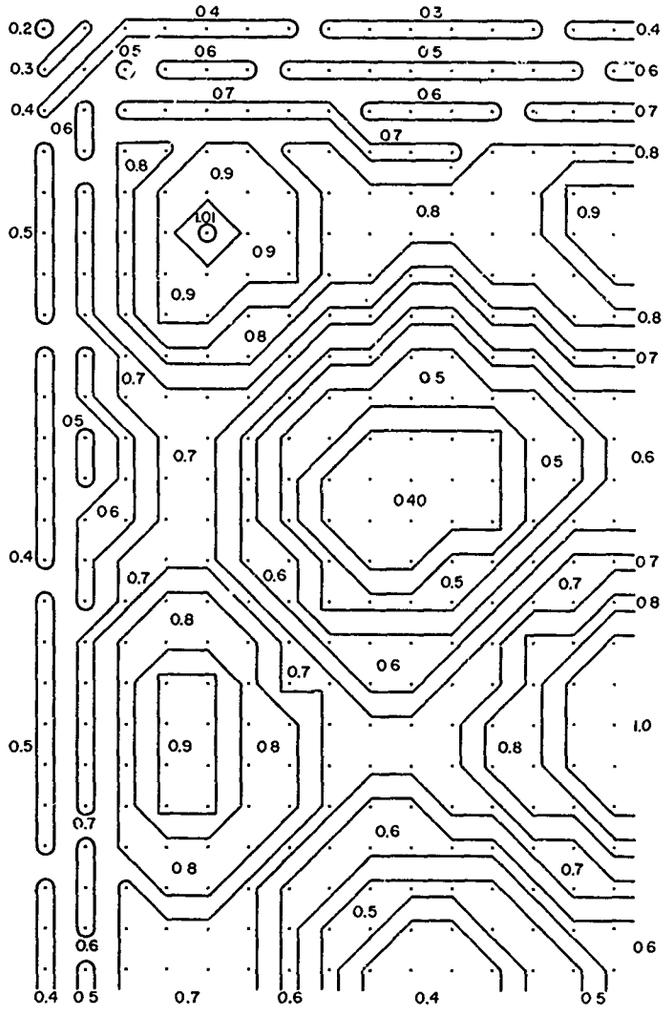

Fig. 24 - Real part of the radiation load on one quadrant of a uniform-velocity array

Since the power limitation for these elements is imposed by fatigue of the element springs, the maximum allowable electrical power input can be extrapolated from the maximum observed deflection at a known input power at each frequency. Manufacturer's tests and experimental results indicate that a peak-to-peak deflection of 0.01 inch is approximately the maximum safe value. The application of a 3-dB safety factor reduces the maximum value to 0.007 inch. This estimated safety factor is required to allow for the size of the statistical sample and for the transient overshoot when the input signal is pulsed. The power input required to produce a maximum peak-to-peak spring deflection of 0.007 inch is plotted in Fig. 25. The corresponding maximum allowable voltage input to the driving amplifiers is plotted in Fig. 26. Since the voltage gain of the amplifiers is adjustable, the input voltage is given as a relative value referenced to the maximum allowable voltage at 380 Hz for the particular amplifier gain employed during the test. The amplifier input-output relations were obtained with a constant voltage input over the frequency range to two amplifiers connected in parallel to the transducer load. The data plotted in Fig. 26 have been extrapolated to the value required to produce the maximum allowable input power at each frequency.

At the conclusion of the experiments an endurance run was conducted consisting of 2 accumulated hours of operation each at frequencies of 350, 415, 430, and 450 Hz with power levels of 200, 400, 300, and 120 kW electrical input, respectively. The power levels employed were based on preliminary analysis of the data and were somewhat higher at 430 Hz and 450 Hz than presently recommended. A check of the elements, following the endurance tests, revealed that two elements had been damaged.

When the array was energized with a phase-reversal modulated pseudorandom signal, an examination of the oscillographic records of element mass displacements revealed a very nearly linear relationship between the signal voltage waveform and the external mass displacement. The spring deflections, however, showed no recognizable correspondence. Large peak values of deflection occurred at apparently random intervals in the sequence. Measurements of the maximum excursion of the deflection values indicated that the maximum allowable rms current input is 85 amp. It is recognized that the radiation loading patterns existing with steady-state excitation do not apply for modulated signal waveforms. At the present level of understanding, it is not possible to predict the maximum power level for modulated waveforms from steady-state measurements. Additional experiments (9) conducted during the acoustic calibration tests disclosed that maximum allowable power for pseudorandom signal excitation depends upon a number of variables. The results presented in Table 1 show the variation in allowable power into the array for 12 different modulated signal types. All the signals employed were pseudorandom in some sense, but they differed from each other in the following respects:

Center frequency	380, 400, 420 Hz
Modulation frequency	100, 80, 50, 42 Hz
Filtering	350-450 Hz, 350-430 Hz
Method of modulation	PM, FSK, PRN

The phase-modulated (PM) signals were obtained by using a shift register output to coherently phase modulate a carrier frequency f_0. The carrier phase was zero or 180 degrees, depending upon whether the shift register output was zero or one. The center frequency could be changed from the normal value of 400 to 380 Hz or to 420 Hz, and the filters at the output could be changed to pass the band from 350 to 450 Hz or from 350 to 430 Hz. The modulation frequency could also be varied by changing the shift register

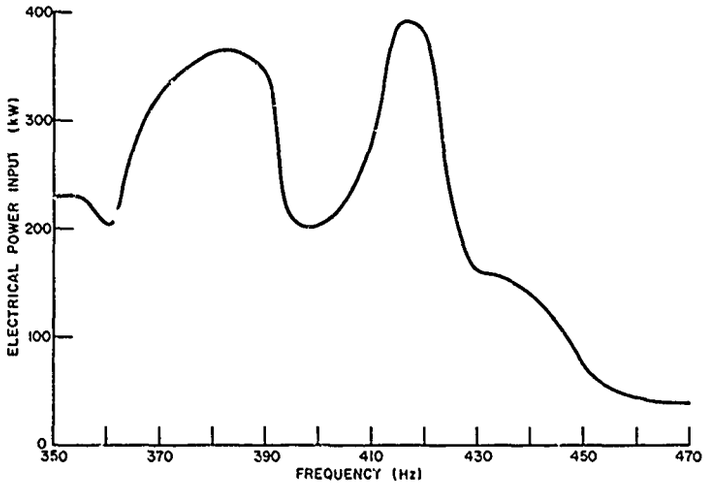

Fig. 25 - Maximum allowable power input to the completed Artemis array for pulsed sinusoids

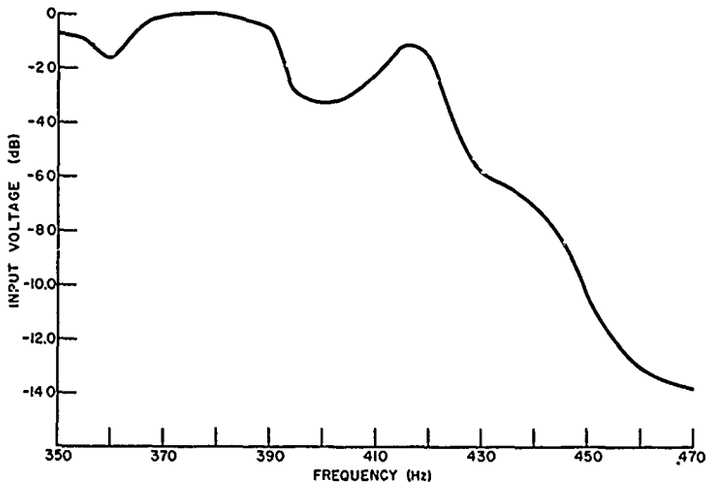

Fig. 26 - Relative maximum allowable voltage input to the completed Artemis source for pulsed sinusoids

rate from 100 to 80 Hz or to 50 Hz, thus changing the length (in cycles) of the signal bit from four to five and eight, respectively. The frequency shift keying signal (FSK) was modulated by the same shift register, but the modulation process consisted of shifting the carrier frequency between 380 and 420 Hz in a phase-coherent manner. The pseudorandom noise (PRN) signal was generated by the NRL pseudonoise generator, which is a shift register operating at a 3.2-kHz clock rate. A 100-Hz band centered at 400 Hz was selected by filtering the generated signal. In a second mode of operation, the filtered signal was clipped and filtered again through a 100-Hz bandpass filter, resulting in a lower peak-to-rms ratio.

Table 1
Allowable Power Input for Various Modulated Signals

Number	Modulation Type*	Shift Reg. Length	Modulation Rate (Hz)	Center Freq. (Hz)	Filter Bandwidth (Hz)	Allowable Power (kW)
1	PRS	12	100	400	350–450	182
2	PRS	12	100	400	350–430	232
3	PRS	12	100	380	350–450	262
4	PRS	12	100	420	350–450	229
5	PRS	7	100	400	350–450	245
6	PRS	12	80	400	350–450	257
7	PRS	11	50	380	350–450	268
8	PRS	11	50	420	350–450	307
9	PRS	11	50	400	350–450	342
10	PRN	–	wide band	400	350–450	110
11	PRN clipped and filtered	–	100	400	350–450	237
12	FSK	11	42	400	350–450	385

*PRS = Phase reversal modulated pseudorandom signals; PRN = NRL pseudorandom noise signals; FSK = frequency-shift keying.

The allowable power tabulated in Table 1 is the maximum allowable power based on the largest spring deflection of any sampled element. One trend evident in the table indicates that, for a given center frequency and modulation, the allowable power increases as the bandwidth decreases. This and other relationships in the tabulated results, such as those concerning center frequency and shift register length, are difficult to explain and indicate a need for further investigation of the simultaneous effects of signal waveform, element response, and acoustic interactions. However, the results do illustrate a strong dependence of allowable power input on signal characteristics.

It is interesting to compare the performance of the Artemis array with the performance of one element represented by its electrical analog equivalent circuit. Such a comparison is shown in Fig. 27. The upper broken curve represents the allowable continuous-wave input power to one element, assuming constant acoustic loading of unity ρcA. The lower broken curve represents the allowable continuous-wave power into the element when the worst-case acoustic loading situation at each frequency is chosen. The worst-case condition is determined by varying the real and imaginary parts of the acoustic radiation impedance over the range estimated for the Artemis source (zero to 1.0 ρcA for the real part and -0.3 to $+0.3$ ρcA for the reactive part). The solid line represents

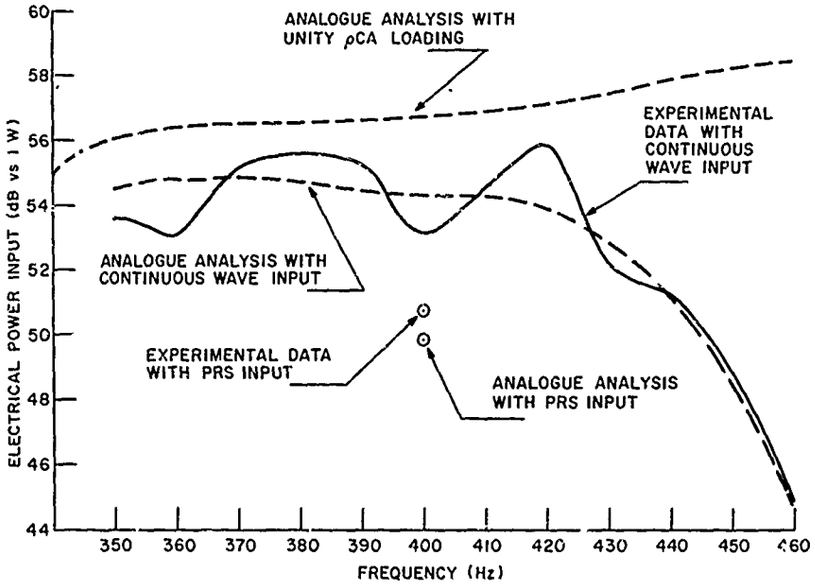

Fig. 27 - Comparison of allowable power for the Artemis array and one analog equivalent element

the curve of maximum allowable input power determined from experimental measurements with specially instrumented elements in the complete array in the field. The dip in the experimental curve at 400 Hz results from the excitation of a rotary mode of vibration in the element. This exemplifies a shortcoming in the analog circuit analysis, since the equivalent circuit did not include this degree of freedom. The experimental and analog curves are in reasonable agreement otherwise, when it is considered that they are both subject to inherent errors. The principal uncertainty in the experimental curve results from the small size of the statistical sample of elements; i.e., approximately 10% of the elements were instrumented. On the other hand, the analog data suffer from the lack of certainty concerning the range and combination of real and imaginary components of acoustic loading values and the approximation of the equivalent circuit to the actual element. A similar analysis was made using phase-modulated pseudorandom signals. The maximum allowable PRS powers, as determined from experimental measurements on the array and from the analog circuit tests with the assumed loading, are plotted as points in Fig. 27. It can be seen that the two methods agree within 1 dB. This is a surprisingly good agreement considering that only fixed loads, whose range of values was derived from steady-state computations, were used. Further studies concerning the nature of transient loading effects are needed before conclusions can be drawn regarding the adequacy of this technique.

Acoustic Calibration

Field Patterns - Acoustic field measurements were obtained using three hydrophones mounted on a spar attached to a 190-foot boom. The boom was provided with a latching mechanism to insure positional accuracy of the hydrophones. Three latched positions were provided which, with the three hydrophones, gave nine fixed measurement

points at depression angles relative to the acoustic axis of: -2.5, 0, 2.5, 5, 7.5, 10, 17.5, 20, and 22.5 degrees. Some additional measurements were made at intermediate non-latched positions. Details of the measurement technique will be found in Ref. 9.

The ranges of the hydrophones from the center of the array varied from 189.2 to 199.9 feet, depending on the boom position. These ranges are not sufficient to yield true far-field results. However, this range yields an adequate approximation for angles within 10 degrees of the acoustic axis. An indication of the validity of the approximation to far-field conditions is given by the results of computations in which the Artemis source was represented by a field of 160 point-source radiators uniformly spaced over the dimensions of the array and driven in phase. The amplitude and phase of the acoustic field of the point-source array were computed for hydrophone ranges of 190 feet and infinity. The results of these computations at 400 Hz are plotted in Fig. 28 along with the measured field of the Artemis array. The far-field amplitude is normalized to zero on the acoustic axis. Phase is referred to zero range to the center of the array. The amplitude pattern computed at hydrophone range is within 0.5 dB of the far-field pattern for all angles in the major lobe out to approximately 9.5 degrees. For larger angles, particularly those near the null, the difference becomes large. The phase angles computed for a range of 190 feet and for far field show an appreciable difference for all angles. However, the phase difference is shown in Ref. 9 to be a linear function of frequency and thus appears as a time shift and does not produce distortion. It can be seen from Fig. 28

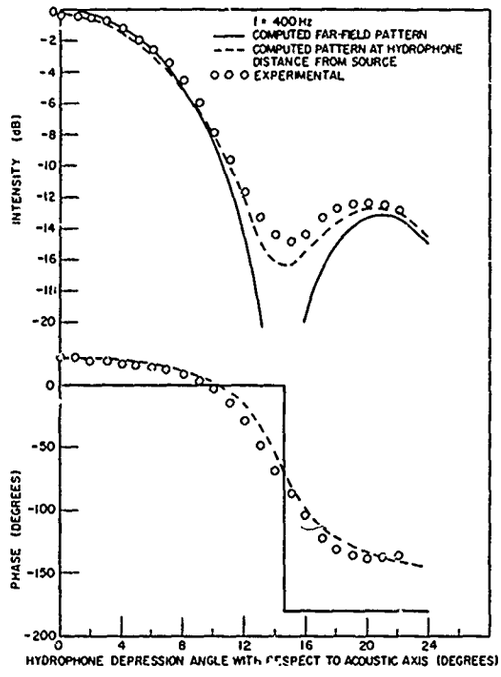

Fig. 28 - Experimental and computed field patterns at 400 Hz

that the amplitude and phase patterns measured on the Artemis array agree well with the near-field computed patterns; therefore it can be concluded that this array pattern resembles that of a uniformly vibrating piston.

Figure 29 is a polar plot of the measured amplitude patterns at 350, 400, and 450 Hz. At each frequency the amplitude plots are normalized to the on-axis values. Figures 30a through 30g present amplitude and phase data on expanded linear scales for seven frequencies between 300 and 500 Hz. In these plots both amplitude and phase are normalized to the on-axis values. The 3-dB beamwidth is seen to range from 11 to 15 degrees over the bandwidth from 450 to 350 Hz.

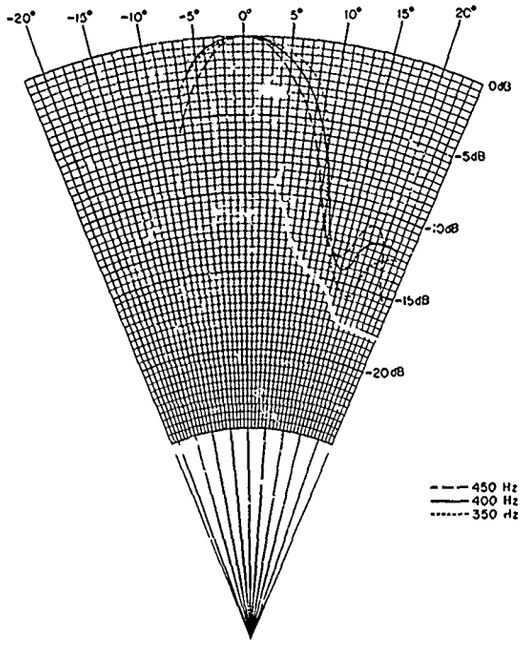

Fig. 29 - Polar plot of field patterns at 350, 400, and 450 Hz

On-axis source levels at 1 yard for various current levels are shown in Fig. 31. Figure 32 gives the source levels for unit power, current, and voltage into the array.

The maximum obtainable source levels, based on the maximum allowable input power curve of Fig. 25 and the response curves of Fig. 32, are shown in Fig. 33 as a function of frequency. The corresponding maximum allowable power and voltage curves (Figs. 25 and 26) are reproduced in this figure for comparison purposes.

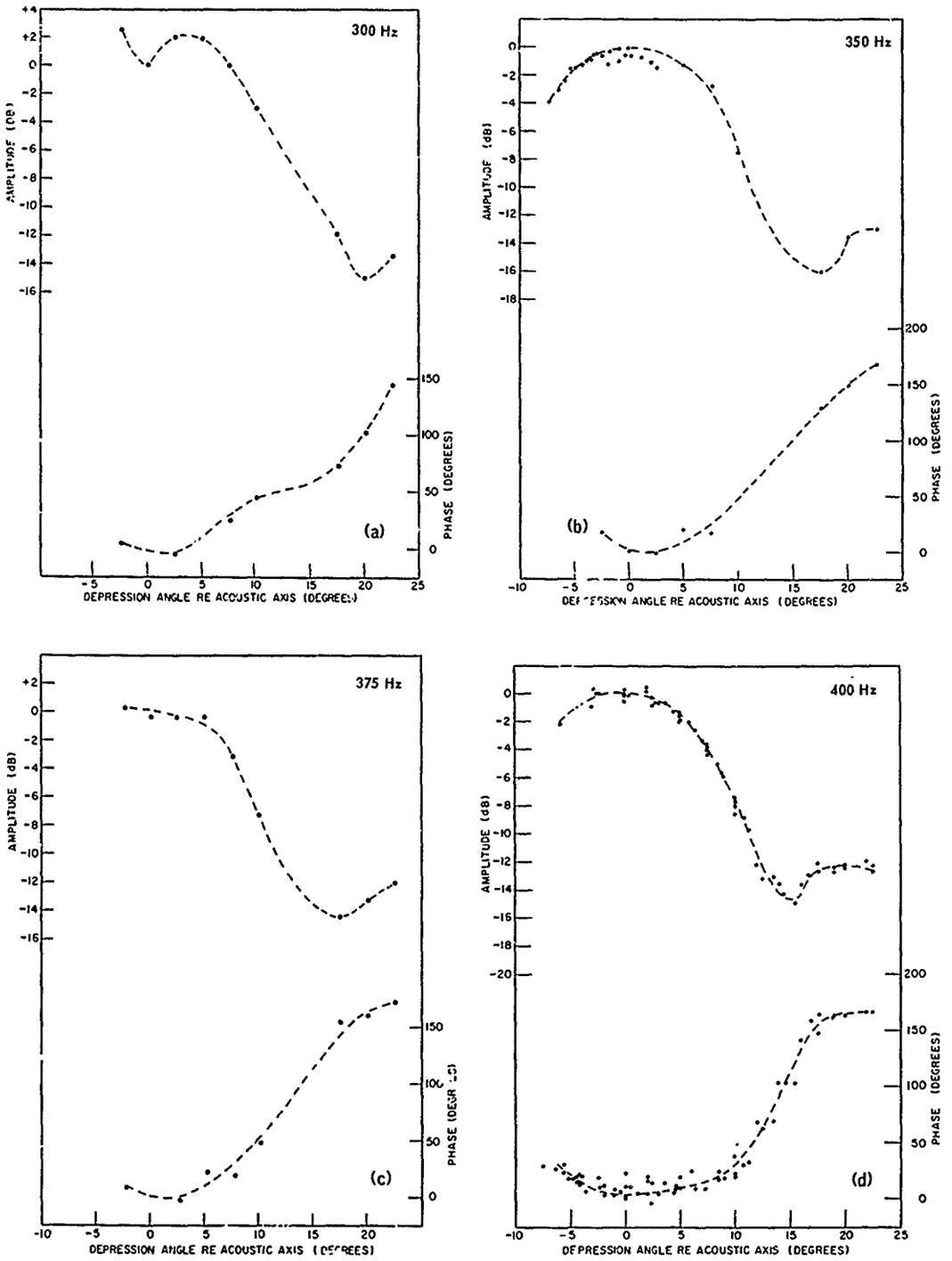

Fig. 30 - Acoustic field pattern with amplitude and phase normalized to the on-axis values—Continued

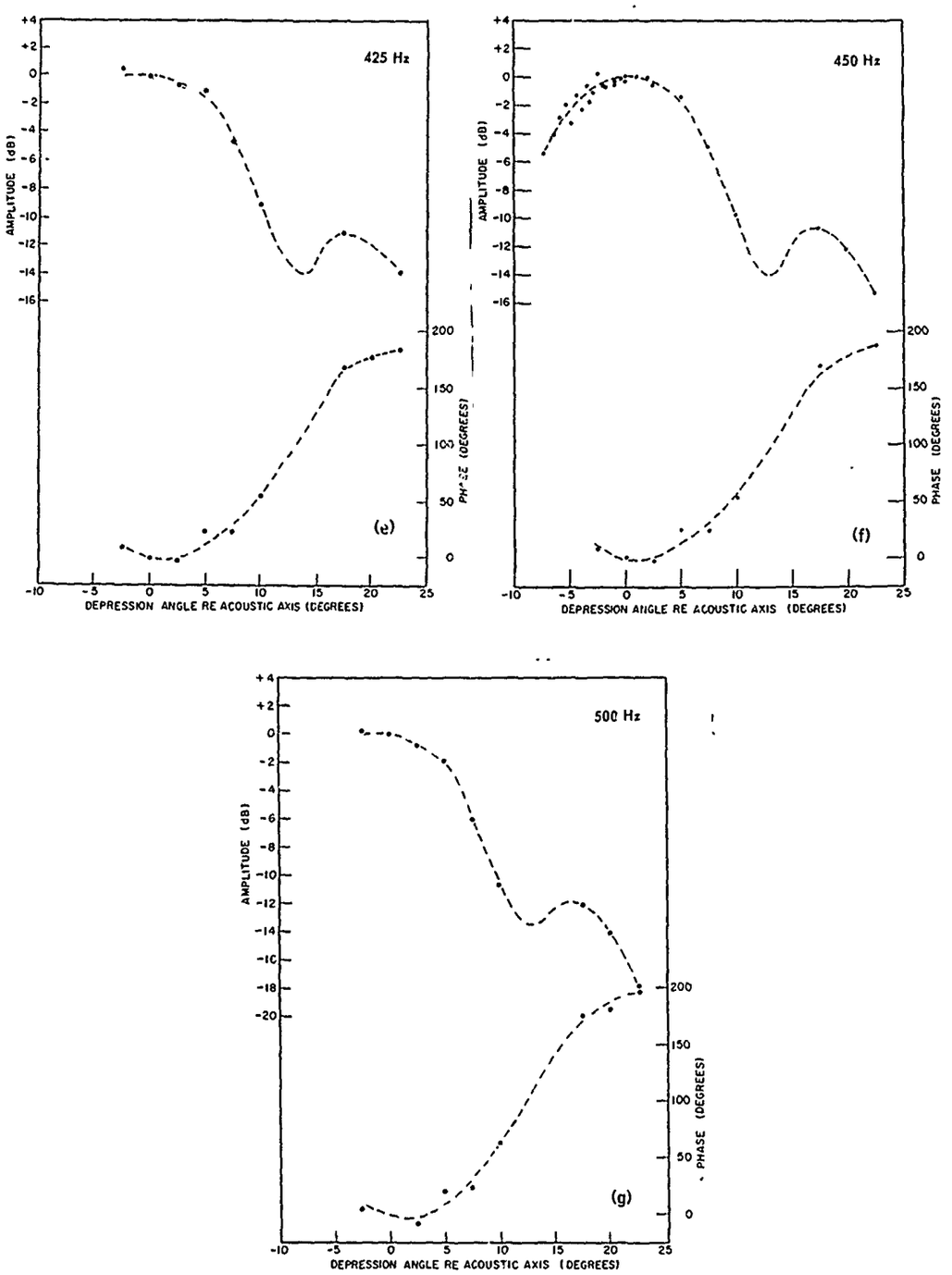

Fig. 30 - Acoustic field pattern with amplitude and phase normalized to the on-axis values

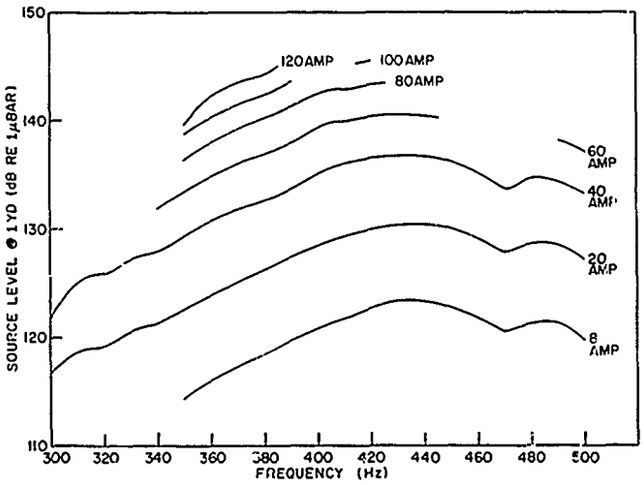

Fig. 31 - On-axis cw source levels at 1 yard

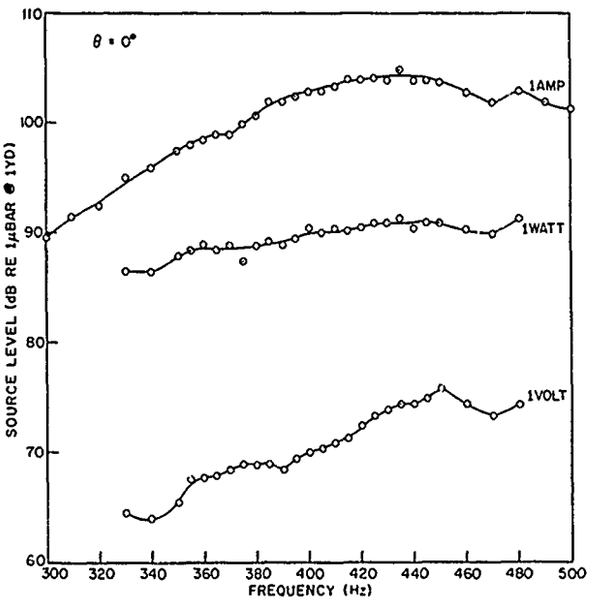

Fig. 32 - On-axis cw source levels per ampere, per watt, and per volt

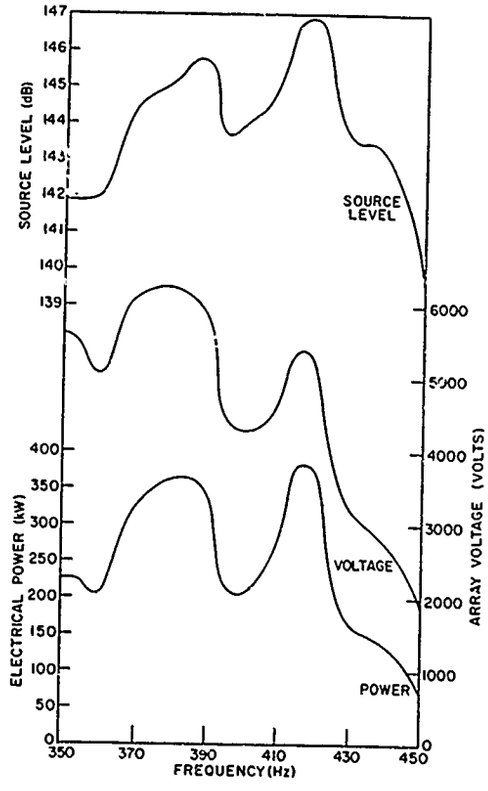

Fig. 33 - Maximum allowable cw source level, vs frequency, on axis, with corresponding voltage and power

Transfer Function Results - The transfer function is defined as

$$H_\theta(\omega) = \frac{V_{h_\theta}(\omega)}{V'_G(\omega)} = \frac{V_{0_\theta}(\omega)\, e^{-j\omega\tau_p}}{V_G(\omega)\, e^{-j\omega\tau_p}} = \frac{V_{0_\theta}(\omega)}{V_G(\omega)},$$

where

θ = the depression angle relative to the acoustic axis,

V_{h_θ} = the voltage of the hydrophone at depression angle θ and range R,

V_{0_θ} = the hydrophone voltage V_{h_θ} referred to zero range,

V_G = the signal generator voltage (input to the Artemis amplifier console),

τ_p = the acoustic propagation delay = R/c, and

V'_G = the signal generator voltage delayed by the propagation time.

In the instrumentation system, the signal generator voltage V_G was delayed by τ_p seconds, and the phase of V_{h_θ} relative to V'_G was measured, since it equaled the desired phase of V_{0_θ} relative to V_G. Thus, the transfer function obtained is the ratio of the far-field signal in the water (at beam angle θ) to the console input signal, with the propagation delay eliminated.

These measurements (9) were made using sine wave excitation and also using PRS excitation with amplitude and phase measurements made in contiguous 4-Hz bands. The PRS signals were generated using a linear shift register with shift rates of 50 and 100 Hz. The 50-Hz shift rate was used with an 11-bit register and the 100-Hz rate with a 12-bit register to produce a signal length of 42 seconds in each case. The shift register output caused a 180-degree phase shift in the 400-Hz carrier, thus producing a signal with a 400-Hz center frequency and pseudorandom phase-reversal modulation. The 11-bit register code (12) was 5205E and the 12-bit code was 10123F. The sine wave results are plotted in Figs. 34a through 34i for each of the hydrophone positions (θ = -2.5, 0, 2.5, 5, 7.5, 10, 17.5, 20, and 22.5 degrees). These results were obtained at 40 amp rms amplifier output. Linearity considerations are discussed in a later section. It should be noted that all transfer function measurements were made with the console filter out, and that there is a 180-degree phase shift in the amplifier input circuits. The transfer function measurements were made with a 12.4 μF tuning capacitor bank connected in series with the amplifier output.

The 0, 7.5, and 20 degree transfer function results obtained using PRS excitation at a level of 80 amp rms are plotted in Figs. 35 and 36. The amplitude data is normalized to zero dB on axis at 400 Hz. The 80-amp continuous wave results are plotted for comparison. It can be seen that the results agree to within 1 dB in amplitude and 10 degrees in phase. Another significant characteristic of the transfer function results is that the amplitude characteristic over the band from 350 to 450 Hz is flat within ± 1.5 dB, and the phase characteristic is very nearly linear with frequency for the major lobe. The phase characteristics are replotted in Fig. 37 with linear phase shifts removed so that the phase in each case is zero degrees at 400 Hz. The phase characteristic is seen to be essentially flat for both PRS and cw signals over the band from 350 to 450 Hz.

The coherence ratios, derived from the cross-power spectral densities used in transfer function measurements, were computed for each hydrophone position as follows:

$$\text{coherence ratio } \gamma = \frac{|S_{xy}(\omega)|^2}{S_{xx}(\omega) \cdot S_{yy}(\omega)},$$

where

$S_{xy}(\omega)$ = the cross-power spectral density between input and output,

$S_{xx}(\omega)$ = the input power spectral density, and

$S_{yy}(\omega)$ = the output power spectral density.

The coherence ratios are unity to within the experimental error of the measurements (approximately ± 2%), with the exception of the far off-axis results which show some real deviation from unity ratio.

Crosscorrelation Measurements - Crosscorrelation measurements (9) were made between each hydrophone signal and the PRS generator. The signals used were the same as those employed in the transfer function measurement, namely, phase modulated signals of 400-Hz center frequency, and 50 and 100 Hz shift rates. The input level was 80 amp rms. For comparison, the normalized autocorrelation functions for the 50 and 100 Hz shift rate signals are given in Fig. 38.

The instrumentation system measured the crosscorrelation function $R_{xy}(\tau)$ by performing the following operation:

$$R_{yx}(\tau) = \int_0^T y(t)\, x(t-\tau)\, dt,$$

where

y = the hydrophone voltage and

x = the reference signal from the generator.

The normalized crosscorrelation function is obtained by dividing $R_{yx}(\tau)$ by a normalizing factor as follows:

$$\rho_{yx}(\tau) = \frac{R_{yx}(\tau)}{\sqrt{\int_0^T x(t)^2\, dt \int_0^T y(t)^2\, dt}}.$$

The crosscorrelation functions for the on-axis hydrophone are given in Fig. 39 for 50 and 100 Hz modulation rates. These results have been renormalized to let $\rho(0)$ be unity. Thus, the curves can be compared directly with Fig. 38, and it can be seen that there is no measurable difference in curve shape between the autocorrelation functions and the crosscorrelation functions. The peak values of the normalized crosscorrelation functions for both 50 and 100 Hz modulation rates were within ± 5% of unity for all depression angles.

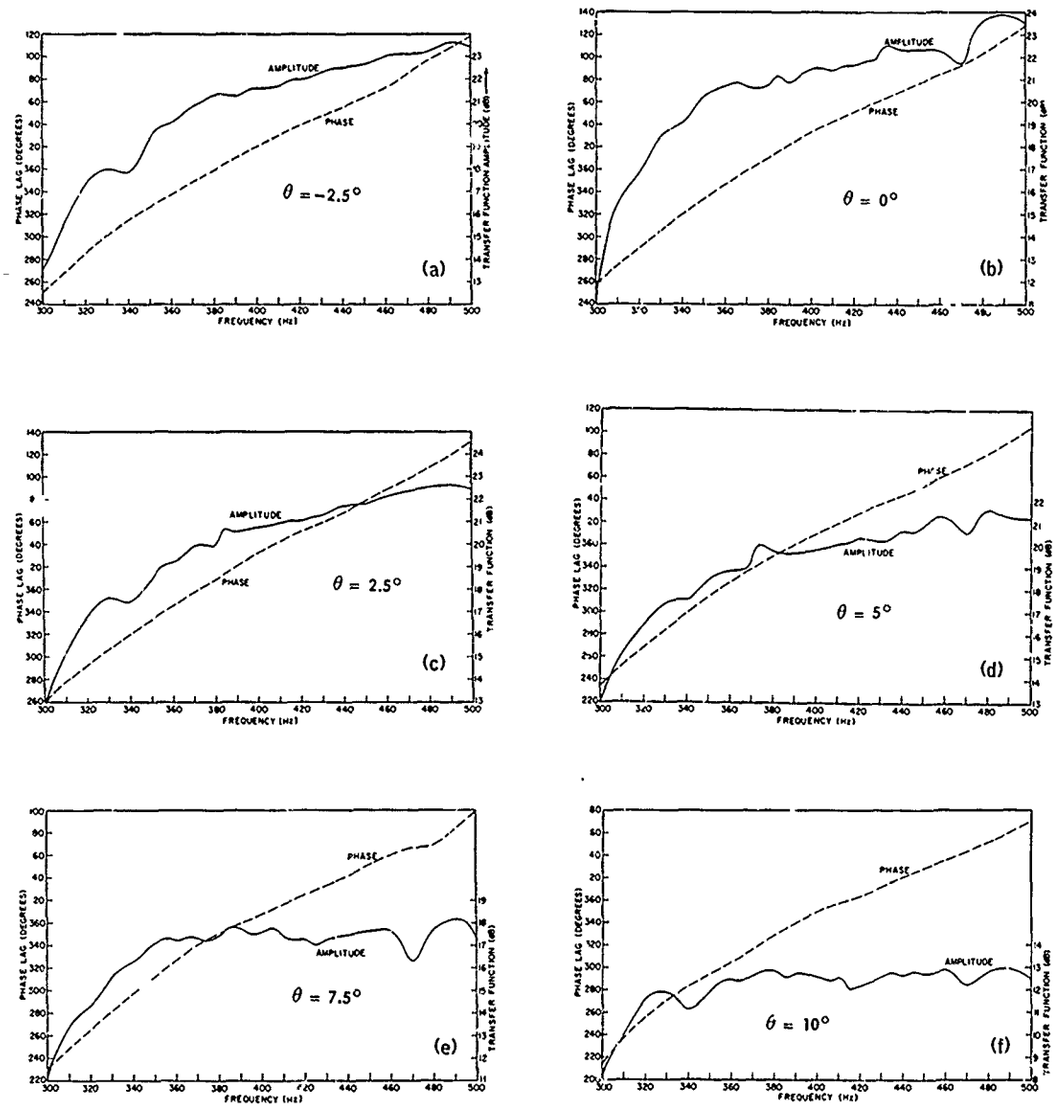

Fig. 34 - Transfer function (amplitude and phase) for continuous-wave measurements at a given depression angle θ—Continued

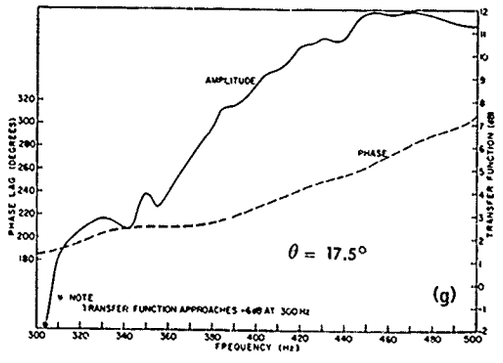

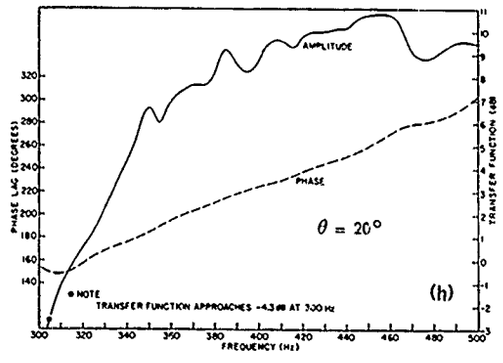

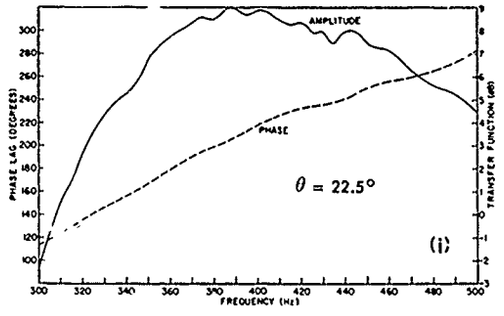

Fig. 34 - Transfer function (amplitude and phase) for continuous-wave measurements at a given depression angle θ

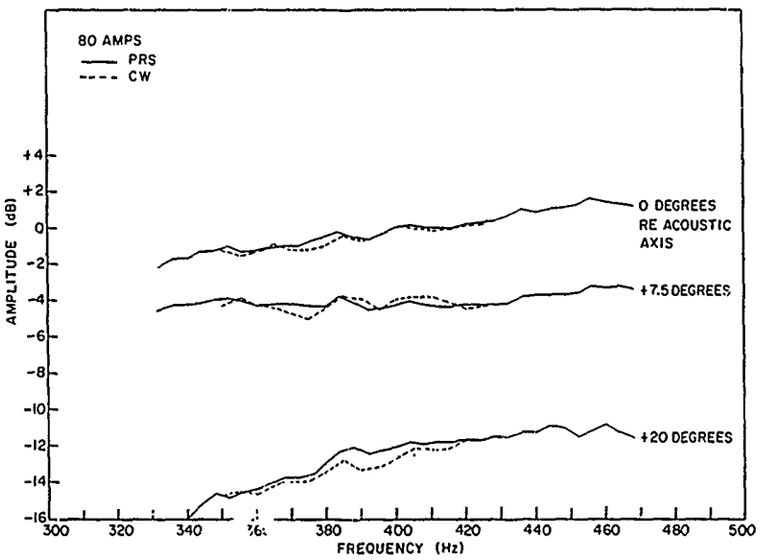

Fig. 35 - Pseudorandom signal and continuous-wave transfer function amplitude

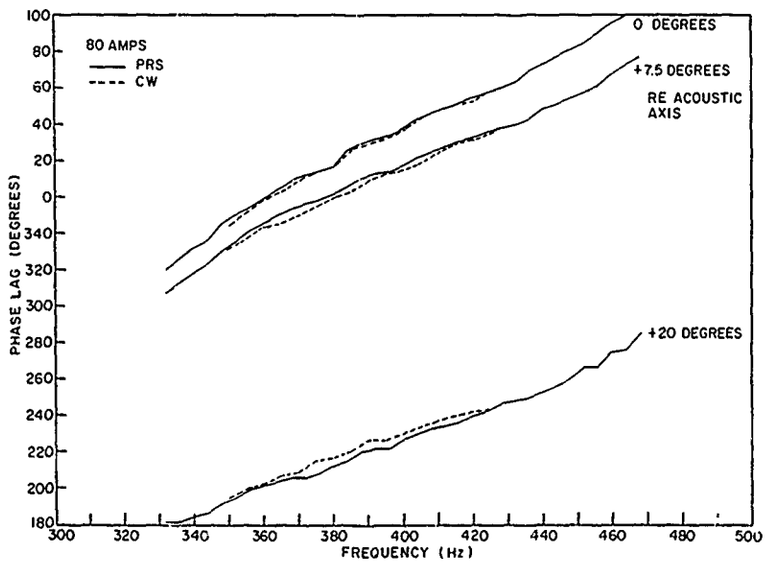

Fig. 36 - Pseudorandom signal and continuous-wave transfer function phase

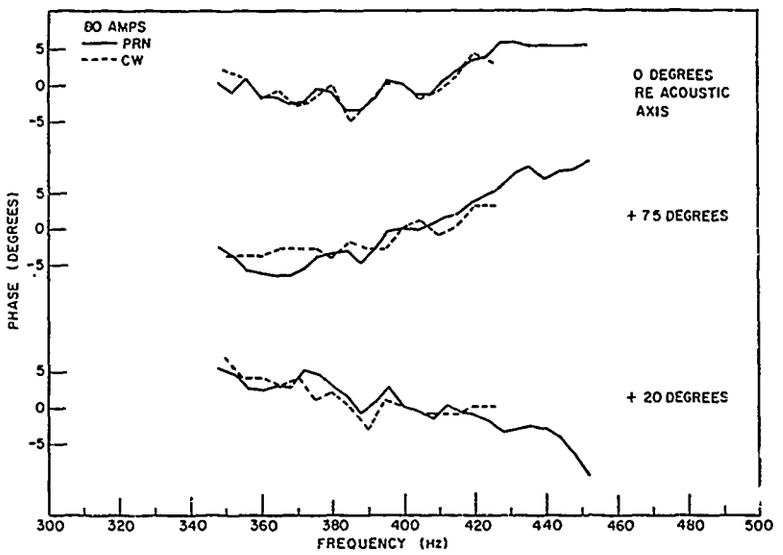

Fig. 37 - Phase comparison of pseudorandom signal and continuous wave with linear component removed

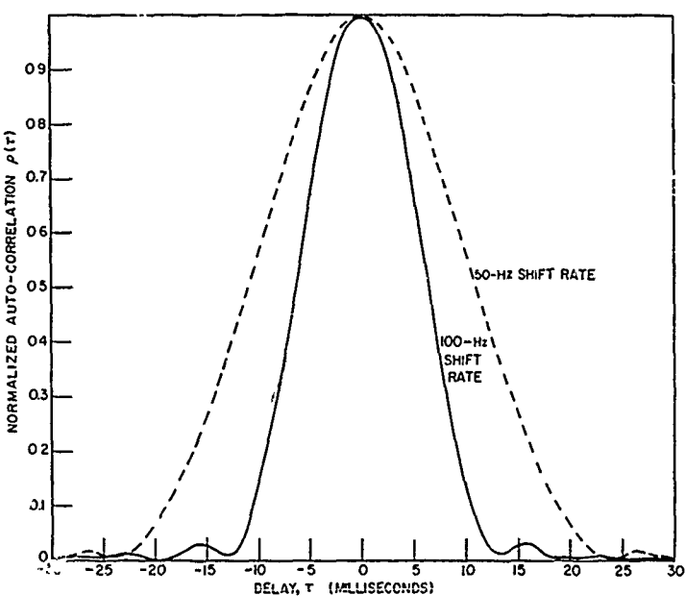

Fig. 38 - Autocorrelation function for 50- and 100-Hz signals

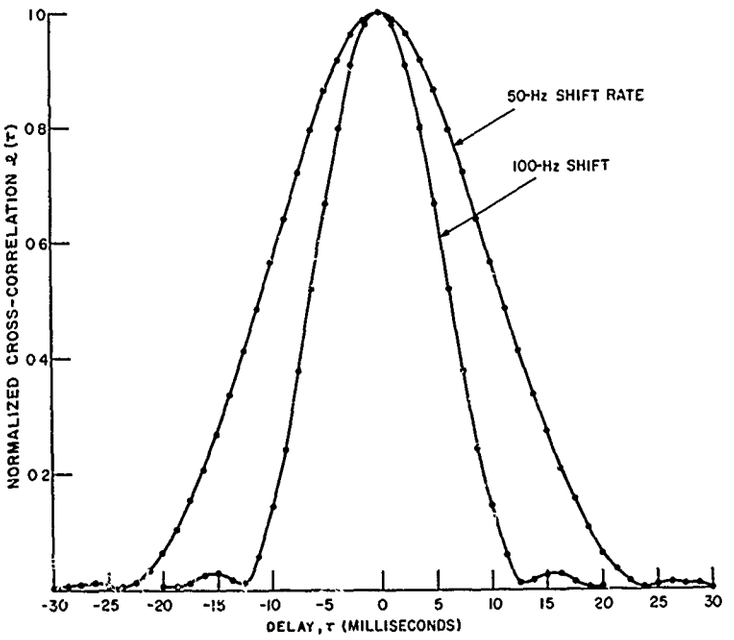

Fig. 39 - Crosscorrelation functions for the 0° hydrophone

Linearity Measurements - The transfer function amplitude and phase for continuous wave excitation were measured at several values of array current. Figure 40 illustrates the results obtained with array currents of 8, 20, and 80 amp. It can be observed that there is an appreciable change in both amplitude and phase with changes in current level. In Fig. 41 phase is plotted as a function of array input current with frequency as a parameter for values of current from 8 amp up to the highest allowable input current for each frequency. Nonlinear behavior is particularly apparent at the lowest frequency, 350 Hz. Figures 42 and 43 illustrate the array impedance as a function of frequency and array input current, respectively. Considerable nonlinearity of array impedance can be observed in Fig. 43. The nonlinearity is also observed in the hydrophone voltage as illustrated in Fig. 44, where the ratios of hydrophone voltage and array input voltage to input current are plotted as a function of array input current. Values have been normalized to unity at an input current of 8 amp. Since the two curves shown in Fig. 44 are in approximate agreement, it can be concluded that the nonlinearity of the hydrophone output is caused principally by the impedance nonlinearity. The data for the curves of Figs. 40 through 44 were obtained with continuous wave excitation. When pseudorandom signals were used the nonlinearity was again observed. The transfer function phases as obtained with cw excitation at 8 amp and at 80 amp array input current are plotted in Fig. 45 together with the PRS transfer function phase at 80 amp. There is a large phase difference between the 8 amp and 80 amp cw data at all frequencies. The 80-amp PRS phase data, however, agrees closely with the 80-amp cw phase data. This is surprising, since the energy in the PRS is spread over a broad band and only a small portion of the energy is contained in the 4-Hz analyzing bandwidth at any one frequency. A similar comparison of PRS and cw amplitude nonlinearity is complicated by several factors and has not been performed. Apparently, the observed phase at any one frequency depends upon the total current into the array and not upon the current in a particular frequency

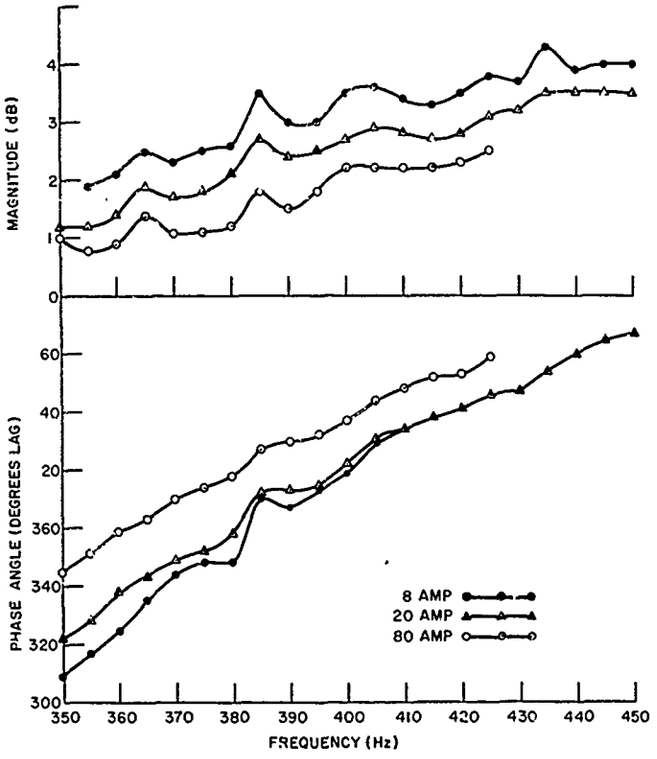

Fig. 40 - Continuous-wave transfer function at 8, 20, and 80 amp

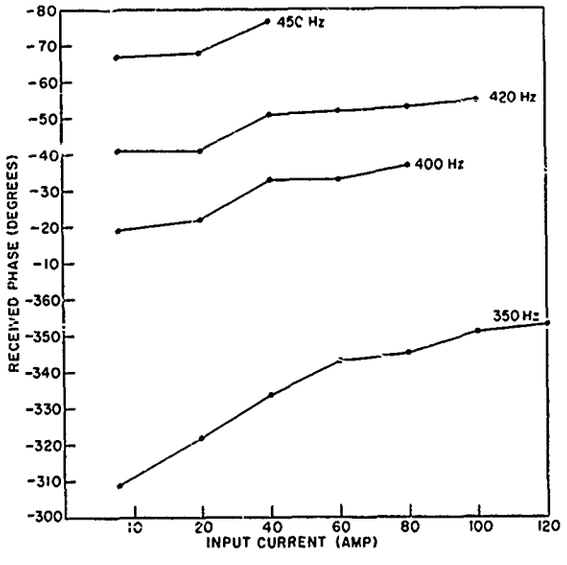

Fig. 41 - On-axis acoustic phase versus array current

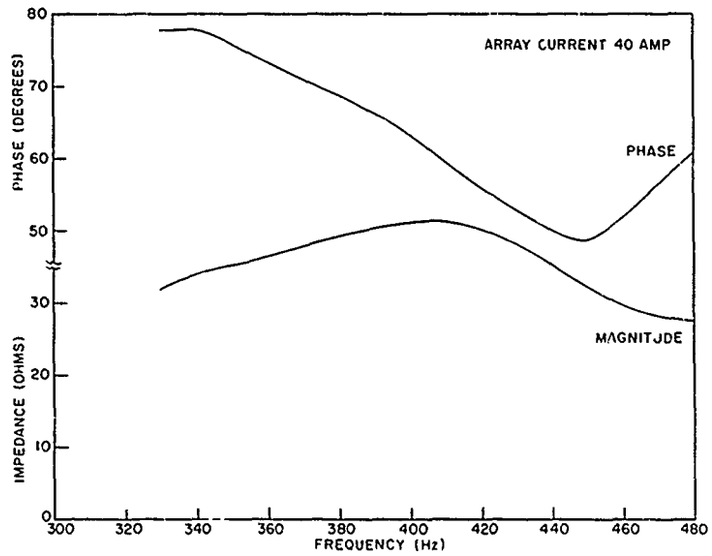

Fig. 42 - Array impedance at 40 amp

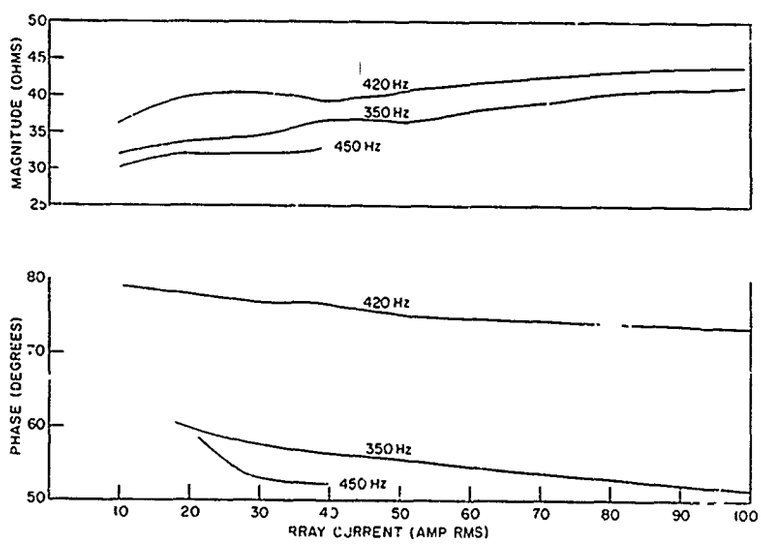

Fig. 43 - Array impedance versus array current

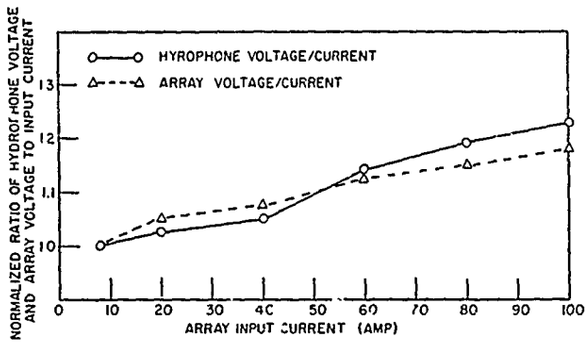

Fig. 44 - Amplitude linearity versus array current at 420 Hz

band. It has been concluded that the observed nonlinearity is caused by an array impedance change which depends upon total current into the array. When operating at a constant current level it would not be expected that nonlinearity, which is dependent upon total input current, would cause waveform distortion. This conclusion is supported by three additional observations:

1. There is no observable waveform distortion in sinusoidal signals received by the hydrophones.

2. The crosscorrelation functions between hydrophone signals and input signals have a peak value of unity.

3. The coherence ratio between hydrophone and input signals is unity.

Thus, it is concluded that the nonlinear characteristics do not introduce measurable distortion in the instantaneous waveforms.

Radiated Noise Spectrum - Table 2 lists all the spectral lines observed over the frequency range of 60 to 15,000 Hz at a hydrophone on the acoustic axis of the source at a range of 190 feet with the array submerged to a depth of 600 feet. The upper section of Table 2 lists the observed lines when the array was energized with 100 amp at 420 Hz. The entries at the bottom of the table are the only lines observed when the array was not energized. Following this test the amplifiers were turned off and the transducer disconnected from the output of the amplifiers. The 420-Hz line disappeared, but the 330-Hz line was unaffected. In computing source levels, it was assumed that the transducer array was the source of all lines except the 330-Hz line, which was assumed to emanate from the ship. It is not known whether the 330-Hz line existed when the array was energized, since only the higher level lines other than harmonics and 60 Hz were recorded at that time. The 330-Hz line represents a source of approximately 1 W acoustic power radiating in a 180-degree solid angle.

At a later date the array was raised to a depth of 155 feet and additional noise measurements were obtained with no excitation to the array. The hydrophone was submerged to a depth of 50 feet at a range of 177 feet from the center of the ship. The ship was assumed to be the source of all lines in the computation of source levels. Table 3 lists all the observed spectral lines. The amplitudes of all lines fluctuated rapidly, unlike the line which was previously observed at 330 Hz, which was steady.

Table 2
Radiated Noise Spectrum With Array Energized
at 420 Hz and With Array Not Energized

Frequency (Hz)	Source Level (dB//1 dyne/cm^2 at 1 yd)	Harmonic
Energized		
60	60.4	
301	80.1	
360	90.0	
420	145.1	Fundamental
480	94.6	
540	86.3	
840	104.5	2nd
1200	64.0	
1260	94.3	3rd
1680	72.3	4th
2100	76.0	5th
2940	70.9	7th
Not Energized		
Amplifier on		
420	82.6	Fundamental
330	75.6*	
Amplifier off		
330	75.6*	

*Source assumed to be ship at range of 600 feet.

Table 3
Radiated Noise Spectrum at 155 Feet With Array Not Energized

Frequency (Hz)	Source Level (dB//1 dyne/cm^2 at 1 yd)	Frequency (Hz)	Source Level (dB//1 dyne/cm^2 at 1 yd)
60	55.4	331	52.9
182	47.4	570	57.4
309	41.4	666	52.9

CONCLUSIONS AND RECOMMENDATIONS

Conclusions

Beam Pattern - Although it is known that the individual elements are subject to widely varying radiation loads and that the velocities of the radiating faces are not uniform, the measured beam patterns agree quite well with the patterns computed on the

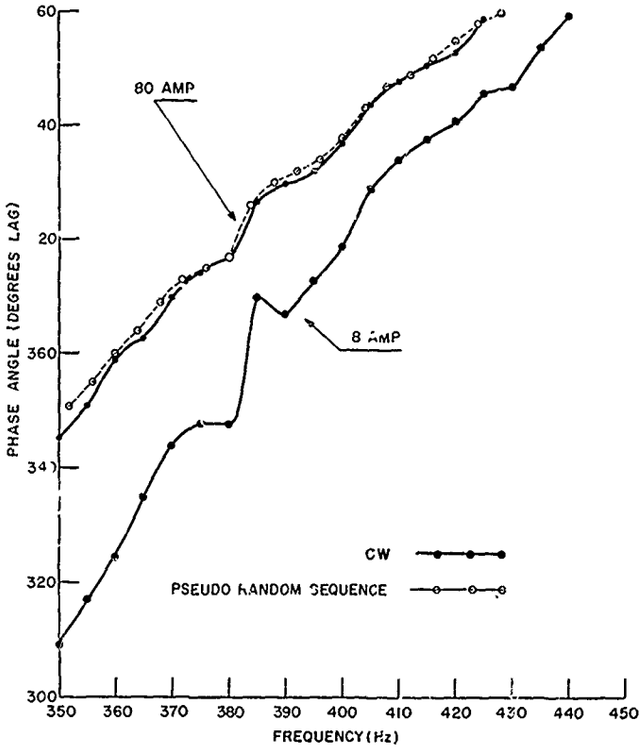

Fig. 45 - Comparison of pseudorandom signal and continuous-wave transfer function at 80 and 8 amp

basis of a uniform velocity assumption. Figure 28 shows the relationship between the experimental beam pattern and a pattern computed using a 160-element uniform-velocity model. While not identical, the actual and ideal curves are in reasonable agreement as to the major and minor lobe characteristics.

Signal Distortion - The correlation measurements obtained at various beam angles indicate that the acoustic signal waveform in the water is an excellent replica of the generator reference signal. No loss of correlation was measurable within the measurement accuracy of the crosscorrelation instrumentation. Since the accuracy of these measurements is estimated to be better than 5%, one can conclude that the generator-to-acoustic-signal correlation is better than 0.95 for the beam angles employed and for the types of signals tested.

Similarly, the close agreement between PRS and cw transfer functions at the same power levels indicates that significant nonlinear behavior of the transducer array does not occur, although there is a dependence of array impedance on total power input. This is supported by the coherence ratios of, essentially, unity.

Source Levels - The cw source levels, as shown in Figs. 31, 32, and 33, are slightly lower than source levels previously reported (8). The maximum allowable source level of 147 dB at 420 Hz, as determined by the more precise measurements of the last test, is 1 dB lower than the result obtained with the acoustic measurements reported in Ref. 8. With modulated signal input, maximum allowable power inputs vary widely depending on many factors (cf. Table 1). For pseudorandom noise signals generated by the NRL PRN generator the maximum allowable power input is 110 kW, whereas a signal specially designed for maximum power (phase coherent FSK) has a maximum allowable power input of 385 kW, which is nearly identical to the maximum allowable power for cw excitation. Allowable powers for conventional phase reversal PRS inputs fall between these two values.

The Artemis source contains 1440 massa-type TR-11C transducer elements. These elements have a maximum recommended spring deflection of 10 mils peak to peak. A group of modified elements, having newly designed springs, was tested (13) for 10,000,000 cycles at a spring deflection of 22 mils peak to peak without damage. Mechanical limitations of the air gap prevented testing at larger deflections. The manufacturer, however, had tested the individual springs at 44 mils peak to peak deflection. If the Artemis source was to be equipped with elements containing the modified springs, an increase in the maximum allowable power of approximately 12 dB could be expected, provided the transducer element remained the power limiting factor.

Suggested Areas For Further Investigation

Acoustic Interaction Effects - Experience with the Artemis source has shown that acoustic interaction effects are significant in terms of maximum power capability, although the beam patterns and transfer functions are apparently not adversely affected. The effect of acoustic interaction is particularly difficult to estimate when modulated signals are employed. Further investigation into the radiation loading of individual elements in arrays excited by modulated waveforms is indicated.

Element Design Criteria - The extreme spread of spring deflections in the Artemis elements over the array under cw excitations, and the large responses of individual elements when excited by modulated waveforms, indicate that additional criteria related to dynamic response should be incorporated in design specifications. There is need for investigation of optimum relationships between signal bandwidth, transduction efficiency, transducer Q, maximum power capability, radiation loading effects, and signal distortion.

Array Measurement and Evaluation Methods - The problems associated with performance measurements on large, low-frequency arrays are formidable. Near field measurement techniques would be helpful. It is also desirable to establish some standard way of evaluating array performance under conditions of excitation by modulated waves for comparison purposes and for acceptance testing.

System Response to Modulated Waveforms - The previous three paragraphs have indicated the importance of additional investigation employing modulated waveforms. It is to be stressed that designs based on continuous-wave sinusoidal assumptions are not adequate for use with high-power acoustic arrays which will be used with various types of modulated signals.

REFERENCES

1. McClinton, A.T., Ferris, R.H., Cybulski, J., and Barton, A.M., "Project ARTEMIS High Power Acoustic Source, Description of Facility as Installed on *USNS Mission Capistrano* (T-AG 162)," NRL Report 5599 (Confidential Report, Unclassified Title), Feb. 1961 and Supplement of July 1961

2. McClinton, A.T., "Project ARTEMIS Acoustic Source, Description and Characteristics of Facility as Installed on the *USNS Mission Capistrano* (T-AG 162)," NRL Memorandum Report 1299 (Confidential Report, Unclassified Title), Mar. 1962

3. McClinton, A.T., Ferris, R.H., Herrington, W.A., "Project ARTEMIS High Power Acoustic Source, Interim Report on Acoustic Performance," NRL Memorandum Report 1205 (Confidential Report, Unclassified Title), Aug. 1961

4. McClinton, A.T., Ferris, R.H., "Project ARTEMIS High Power Acoustic Source, Second Interim Report on Acoustic Performance," NRL Memorandum Report 1214 (Confidential Report, Unclassified Title), Sept. 1961

5. McClinton, A.T., Ferris, R.H., "Project ARTEMIS High Power Acoustic Source, Third Interim Report on Acoustic Performance," NRL Memorandum Report 1273 (Confidential Report, Unclassified Title), Apr. 1962

6. Ferris, R.H., "Project ARTEMIS High Power Acoustic Source, Fourth Interim Report on Acoustic Performance," NRL Memorandum Report 1400 (Confidential Report, Unclassified Title), Mar. 1963

7. Baier, R.V., "Theoretical Interaction Computations for Transducer Arrays, Including the Effects of Several Different Types of Electrical Terminal Connections," NRL Report 6314 (Confidential Report, Unclassified Title), Oct. 1965

8. Ferris, R.H., "Test of Project ARTEMIS Acoustic Source," NRL Memorandum Report 1648 (Confidential Report, Unclassified Title), Sept. 1965

9. Ferris, R.H., Rollins, C.R., "Project ARTEMIS Acoustic Source, Acoustic Test Procedures," NRL Memorandum Report 1769 (Confidential Report, Unclassified Title), in preparation (to be printed)

10. Rusby, J.S.M., "An Investigation of the Total Radiation Impedance of Ridged Piston Sound Sources in Arrays," Part V, Admiralty Research Laboratory Report A.R.L./R31/L (Confidential Report), Sept. 1961

11. Carson, D.L., Martin, G.E., Genthien, G.W., and Hickman, J.S., "Control of Element Velocity Distributions in Sonar Projector Arrays," Proceedings of Seventh Navy Science Symposium, Office of Naval Research Report ONR 16, Vol. I (1963)

12. Peterson, W.W., "Error-Correcting Codes," Cambridge: MIT Press, 1961

13. Ferris, R.H., "Project ARTEMIS Acoustic Source, Characteristics of the Type TR-11F Transducer Element," NRL Memorandum Report 1498 (Confidential Report, Unclassified Title), Jan. 1964

CONFIDENTIAL
Security Classification

DOCUMENT CONTROL DATA - R & D
(Security classification of title, body of abstract and indexing annotation must be entered when the overall report is classified)

1 ORIGINATING ACTIVITY (Corporate author)
Naval Research Laboratory
Washington, D.C. 20390

2a. REPORT SECURITY CLASSIFICATION
Confidential

2b GROUP
4

3 REPORT TITLE
PROJECT ARTEMIS ACOUSTIC SOURCE PERFORMANCE CHARACTERISTICS

4 DESCRIPTIVE NOTES (Type of report and inclusive dates)
An interim report on a continuing problem.

5 AUTHOR(S) (First name, middle initial, last name)
R.H. Ferris and C.R. Rollins

6 REPORT DATE	7a. TOTAL NO OF PAGES	7b. NO OF REFS
June 15, 1967	52	13

8a. CONTRACT OR GRANT NO	9a ORIGINATOR'S REPORT NUMBER(S)
NRL Problem S02-11	NRL Report 6534
b. PROJECT NO. ONR RS 046	
c.	9b. OTHER REPORT NO(S) (Any other numbers that may be assigned this report)
d.	

10 DISTRIBUTION STATEMENT
None

11. SUPPLEMENTARY NOTES	12. SPONSORING MILITARY ACTIVITY
	Department of the Navy (Office of Naval Research), Washington, D.C. 20360

13. ABSTRACT [Confidential]

The Artemis acoustic source was designed to meet the requirements for an ocean surveillance study program. These requirements included a source level of 152 dB in a 100-Hz band centered at 400 Hz with a transducer operating depth of 1200 feet. The transducer, which was completed in June 1964, is a rectangular planar array 33 feet wide and 50 feet high. It is composed of 1440 variable-reluctance elements which are driven in parallel from a linear electronic amplifier. The source is installed aboard a modified T-2 class tanker having a well amidship through which the transducer array is lowered and retrieved.

Initial tests of the partially completed source had revealed a severe acoustic interaction problem which imposed a restriction on the operating power level. A study program was initiated and experiments were conducted to investigate the interaction behavior and to discover means to alleviate its effects. Results demonstrated that improved performance could be obtained by modifying the original series-parallel connection of elements to an all-parallel form. The indicated modification was performed concurrent with the completion of the transducer array.

(over)

14 KEY WORDS	LINK A		LINK B		LINK C	
	ROLE	WT	ROLE	WT	ROLE	WT
Acoustic calibration						
Acoustic field						
Acoustic interaction						
Planar array						
Response characteristics						
Transducer						
Transfer function						

Measurements performed on the completed and modified transducer resulted in a set of recommended safe power levels which depend upon frequency. Operation at the recommended maximum power with pulsed sinusoids at 420 Hz, the favorable frequency, produces a source level of 147 dB referenced to one dyne per square centimeter at one yard. Operation at other frequencies is more limited in power, particularly at the upper end of the frequency band.

An acoustic calibration of the source, accomplished with the aid of hydrophones mounted on the end of a 190-foot boom, defined the transfer function in a vertical plane through the acoustic axis out to the first minor lobe. Correlation functions were obtained between the input signal and the acoustic output using pseudorandom signals. It is concluded that the acoustic source introduces negligible distortion in this type of signal

CONFIDENTIAL

Naval Research Laboratory. Report 6534 [CONFIDENTIAL-Gp-4]. PROJECT ARTEMIS ACOUSTIC SOURCE PERFORMANCE CHARACTERISTICS [Unclassified Title], by R. H. Ferris and C. R. Rollins. 52 pp. and figs., June 15, 1967.

The Artemis acoustic source was designed to meet the requirements for an ocean surveillance study program. These requirements included a source level of 152 dB in a 100-Hz band centered at 400 Hz with a transducer operating depth of 1200 feet. The transducer, which was completed in June 1964, is a rectangular planar array 33 feet wide and 50 feet high. It is composed of 1440 variable-reluctance elements which are driven in parallel from a linear electronic amplifier. The source is installed aboard a modified T-2 class tanker having a well amidship through which the transducer array is lowered and retrieved.

Initial tests of the partially completed source had revealed a severe acoustic interaction problem which imposed a restriction on the operating power level. A study program was initiated and experiments were conducted to investigate the interaction behavior and to discover means to alleviate its effects. Results demonstrated that improved performance could be obtained by modifying the original series-parallel connection of elements to an all-parallel form. The indicated modification was performed concurrent with the completion of the transducer array.

Downgraded at 3 year intervals
Declassified after 12 years

CONFIDENTIAL (Over)

1. Acoustic systems – Calibration
2. Acoustic systems – Test results
I. Ferris, R. H.
II. Rollins, C. R.

CONFIDENTIAL

Naval Research Laboratory. Report 6534 [CONFIDENTIAL-Gp-4]. PROJECT ARTEMIS ACOUSTIC SOURCE PERFORMANCE CHARACTERISTICS [Unclassified Title], by R. H. Ferris and C. R. Rollins. 52 pp. and figs., June 15, 1967.

The Artemis acoustic source was designed to meet the requirements for an ocean surveillance study program. These requirements included a source level of 152 dB in a 100-Hz band centered at 400 Hz with a transducer operating depth of 1200 feet. The transducer, which was completed in June 1964, is a rectangular planar array 33 feet wide and 50 feet high. It is composed of 1440 variable-reluctance elements which are driven in parallel from a linear electronic amplifier. The source is installed aboard a modified T-2 class tanker having a well amidship through which the transducer array is lowered and retrieved.

Initial tests of the partially completed source had revealed a severe acoustic interaction problem which imposed a restriction on the operating power level. A study program was initiated and experiments were conducted to investigate the interaction behavior and to discover means to alleviate its effects. Results demonstrated that improved performance could be obtained by modifying the original series-parallel connection of elements to an all-parallel form. The indicated modification was performed concurrent with the completion of the transducer array.

Downgraded at 3 year intervals
Declassified after 12 years

CONFIDENTIAL (Over)

1. Acoustic systems – Calibration
2. Acoustic systems – Test results
I. Ferris, R. H.
II. Rollins, C. R.

CONFIDENTIAL

Naval Research Laboratory. Report 6534 [CONFIDENTIAL-Gp-4]. PROJECT ARTEMIS ACOUSTIC SOURCE PERFORMANCE CHARACTERISTICS [Unclassified Title], by R. H. Ferris and C. R. Rollins. 52 pp. and figs., June 15, 1967.

The Artemis acoustic source was designed to meet the requirements for an ocean surveillance study program. These requirements included a source level of 152 dB in a 100-Hz band centered at 400 Hz with a transducer operating depth of 1200 feet. The transducer, which was completed in June 1964, is a rectangular planar array 33 feet wide and 50 feet high. It is composed of 1440 variable-reluctance elements which are driven in parallel from a linear electronic amplifier. The source is installed aboard a modified T-2 class tanker having a well amidship through which the transducer array is lowered and retrieved.

Initial tests of the partially completed source had revealed a severe acoustic interaction problem which imposed a restriction on the operating power level. A study program was initiated and experiments were conducted to investigate the interaction behavior and to discover means to alleviate its effects. Results demonstrated that improved performance could be obtained by modifying the original series-parallel connection of elements to an all-parallel form. The indicated modification was performed concurrent with the completion of the transducer array.

Downgraded at 3 year intervals
Declassified after 12 years.

CONFIDENTIAL (Over)

1. Acoustic systems – Calibration
2. Acoustic systems – Test results
I. Ferris, R. H.
II. Rollins, C. R.

CONFIDENTIAL

Naval Research Laboratory. Report 6534 [CONFIDENTIAL-Gp-4]. PROJECT ARTEMIS ACOUSTIC SOURCE PERFORMANCE CHARACTERISTICS [Unclassified Title], by R. H. Ferris and C. R. Rollins. 52 pp. and figs., June 15, 1967.

The Artemis acoustic source was designed to meet the requirements for an ocean surveillance study program. These requirements included a source level of 152 dB in a 100-Hz band centered at 400 Hz with a transducer operating depth of 1200 feet. The transducer, which was completed in June 1964, is a rectangular planar array 33 feet wide and 50 feet high. It is composed of 1440 variable-reluctance elements which are driven in parallel from a linear electronic amplifier. The source is installed aboard a modified T-2 class tanker having a well amidship through which the transducer array is lowered and retrieved.

Initial tests of the partially completed source had revealed a severe acoustic interaction problem which imposed a restriction on the operating power level. A study program was initiated and experiments were conducted to investigate the interaction behavior and to discover means to alleviate its effects. Results demonstrated that improved performance could be obtained by modifying the original series-parallel connection of elements to an all-parallel form. The indicated modification was performed concurrent with the completion of the transducer array.

Downgraded at 3 year intervals
Declassified after 12 years

CONFIDENTIAL (Over)

1. Acoustic systems – Calibration
2. Acoustic systems – Test results
I. Ferris, R. H.
II. Rollins, C. R.

CONFIDENTIAL

Measurements performed on the completed and modified transducer resulted in a set of recommended safe power levels which depend upon frequency. Operation at the recommended maximum power with pulsed sinusoids at 420 Hz, the favorable frequency, produces a source level of 147 dB referenced to one dyne per square centimeter at one yard. Operation at other frequencies is more limited in power, particularly at the upper end of the frequency band.

An acoustic calibration of the source, accomplished with the aid of hydrophones mounted on the end of a 190-foot boom, defined the transfer function in a vertical plane through the acoustic axis out to the first minor lobe. Correlation functions were obtained between the input signal and the acoustic output using pseudorandom signals. It is concluded that the acoustic source introduces negligible distortion in this type of signal. [Confidential Abstract]

CONFIDENTIAL

CONFIDENTIAL

Measurements performed on the completed and modified transducer resulted in a set of recommended safe power levels which depend upon frequency. Operation at the recommended maximum power with pulsed sinusoids at 420 Hz, the favorable frequency, produces a source level of 147 dB referenced to one dyne per square centimeter at one yard. Operation at other frequencies is more limited in power, particularly at the upper end of the frequency band.

An acoustic calibration of the source, accomplished with the aid of hydrophones mounted on the end of a 190-foot boom, defined the transfer function in a vertical plane through the acoustic axis out to the first minor lobe. Correlation functions were obtained between the input signal and the acoustic output using pseudorandom signals. It is concluded that the acoustic source introduces negligible distortion in this type of signal. [Confidential Abstract]

CONFIDENTIAL

CONFIDENTIAL

Measurements performed on the completed and modified transducer resulted in a set of recommended safe power levels which depend upon frequency. Operation at the recommended maximum power with pulsed sinusoids at 420 Hz, the favorable frequency, produces a source level of 147 dB referenced to one dyne per square centimeter at one yard. Operation at other frequencies is more limited in power, particularly at the upper end of the frequency band.

An acoustic calibration of the source, accomplished with the aid of hydrophones mounted on the end of a 190-foot boom, defined the transfer function in a vertical plane through the acoustic axis out to the first minor lobe. Correlation functions were obtained between the input signal and the acoustic output using pseudorandom signals. It is concluded that the acoustic source introduces negligible distortion in this type of signal. [Confidential Abstract]

CONFIDENTIAL

CONFIDENTIAL

Measurements performed on the completed and modified transducer resulted in a set of recommended safe power levels which depend upon frequency. Operation at the recommended maximum power with pulsed sinusoids at 420 Hz, the favorable frequency, produces a source level of 147 dB referenced to one dyne per square centimeter at one yard. Operation at other frequencies is more limited in power, particularly at the upper end of the frequency band.

An acoustic calibration of the source, accomplished with the aid of hydrophones mounted on the end of a 190-foot boom, defined the transfer function in a vertical plane through the acoustic axis out to the first minor lobe. Correlation functions were obtained between the input signal and the acoustic output using pseudorandom signals. It is concluded that the acoustic source introduces negligible distortion in this type of signal. [Confidential Abstract]

CONFIDENTIAL